International Journal of Dynamics and Control (2024) 12:2166–2189
https://doi.org/10.1007/s40435-023-01318-y

Numerical solution of time-fractional telegraph equations using wavelet transform

Mallanagoud Mulimani[1] · **Kumbinarasaiah S**[1]

Received: 26 June 2023 / Revised: 12 September 2023 / Accepted: 18 September 2023 / Published online: 20 November 2023

Abstract
This study solves the time-fractional telegraph equations with Dirichlet boundary conditions using a novel and effective wavelet collocation method based on Taylor wavelets. In the Caputo sense, the fractional derivative idea is used. The Taylor wavelets are created from the Taylor polynomials. The operational matrices of integration are extracted from the Taylor wavelets. The Taylor wavelet method (TWM) is developed using these operational integration matrices. According to this method, the selected telegraph equation is converted into a system of algebraic equations. Newton's iterative technique solves the attained system of algebraic equations. The proposed method's error estimate is provided. The projected method solution is compared with the numerical solutions of Sinc-Legendre, Legendre, and Fibonacci wavelet collocation methods in terms of the tables and graphs. The results obtained from the TWM are accurate and efficient. As we know, many PDEs do not have exact solutions, and some semi-analytical methods work based on controlling parameters, but this technique is free from controlling parameters. Also, it is easy to implement and consumes less time to execute the programs. The suggested wavelet-based numerical method is computationally appealing, successful, trustworthy, and resilient.

Keywords Telegraph equation · Dirichlet boundary condition · Taylor wavelets · Collocation points · Operational matrix · Newton's iterative technique

Mathematics Subject Classification 26A33 · 35G15 · 49M15 · 65N35 · 65T60

1 Introduction

Fractional calculus and its applications effectively express various problems in numerous engineering and scientific disciplines. Many researchers and scientists have recently been interested in fractional calculus. It has been found that fractional models are more precise and efficient than previously introduced classical models and that fractional derivative operators play a significant role in describing physical processes. There are many types of integral and derivative operators such as, including Caputo [1], Grünwald-Letnikov [1], Riemann–Liouville [1], Atangana-Baleanu [2], and Caputo-Fabrizio (CF) [3]. Numerous classes of fractional equations have been used in recent years to model a variety of real phenomena in mechanics, physics, chemistry, biology, medicine, economics, and signal processing, including diffusion and wave propagation, viscoelasticity and damping, image processing, and control systems [4–11]. To simulate many significant occurrences in these sectors by fractional calculus, numerous researchers in many fields of physics, chemistry, biology, mathematics, engineering, and other science have extensively examined these phenomena. Recent research on solved fractional differential equations, which are time-fractional Korteweg-de Vries equation [12], generalized fractional-order differential equations [13], nonlinear fractional differential equations [14], fractional Sawada-Kotera-Ito equation [15], has made it simpler for researchers to understand fractional calculus.

Oliver Heaviside first proposed the telegraph equation, a linear second-order hyperbolic partial differential equation describing the current and voltage on an electricity transmission line with distance and time. The model illustrates the ability of the wire to reflect electromagnetic waves and the formation of wave patterns along the wire [16]. The theory applies to high-frequency and direct current transmission

✉ Kumbinarasaiah S
kumbinarasaiah@gmail.com

[1] Department of Mathematics, Bangalore University, Bengaluru, India

lines of all frequencies. Initially created to describe telegraph wires, the idea also applies to conductors operating at audio frequencies (telephone lines), radio frequencies, low frequencies (power lines), and direct current pulses. They can electrically represent wire radio antennas as shortened single-conductor transmission lines [17, 18]. The telegraph equations can also be used to explain a wide range of phenomena in the chemical, physical, and biological sciences, including acoustic waves in porous media [19], wave propagation in cable transmissions [20], population dynamics [21], parallel flows in Maxwell fluids [22], hyperbolic heat transfer [23], and pulsatile blood flow in arteries [24]. The telegraph equation is frequently applied to studying wave phenomena and the propagation of electric signals in cable transmission lines and to simulate reaction–diffusion processes in various fields like engineering and biological sciences. There are numerous applications in wave propagation and signal analysis, and nobody solved the telegraph equations using the Taylor wavelet. This motivated us to solve the telegraph equations by using Taylor wavelets.

The general form of a nonhomogeneous time-fractional telegraph equation with physical conditions is given by,

$$\frac{\partial^{\delta} X(r,\,t)}{\partial t^{\delta}} + a\frac{\partial^{\delta-1} X(r,\,t)}{\partial t^{\delta-1}} + bX(r,\,t) = c\frac{\partial^{2} X(r,\,t)}{\partial r^{2}} + h(r,\,t),\ (r,\,t) \in \Omega \times \Omega, \tag{1.1}$$

with initial and Dirichlet boundary conditions

$$X(r,\,0) = d_1(r),\ \ X_t(r,\,0) = d_2(r),\ \ r \in \Omega, \tag{1.2}$$

$$X(0,\,t) = g_1(t),\ \ X(1,\,t) = g_2(t),\ \ t \in \Omega, \tag{1.3}$$

where a, b, and c are real constants, $\Omega := [0,\,1]$ and $h(r,\,t)$ is a continuous real-valued function. The parameter δ represents the fractional derivative with $1 < \delta \leq 2$. The fractional telegraph equation becomes the classical telegraph equation when $\delta = 2$.

The solution of differential and integral equations can benefit significantly from using wavelets, another basis set, and highly well-localized functions. Wavelet approaches are more engaging, precise, and reliable in solving integral and differential equations. Wavelet methods are increasingly popular among scholars for resolving partial and fractional differential equations. The data functions or operators are divided into frequency constituents using the powerful and effective mathematical tool called wavelets. Each constituent is then analyzed or studied with a resolution appropriate to its scale. Wavelet theory has drawn much interest recently due to its valuable applications in several fields, including numerical analysis, system analysis, signal analysis, and optimal control [25]. Wavelets are valuable because of their unique characteristics [26]. In particular, the literature frequently employs orthogonal wavelets to handle various differential equations. Several wavelet-based numerical approaches have been magnificently solved in the literature, including the following: Fibonacci wavelet approach [27–33], Legendre wavelet collocation method [34], Hermite wavelet collocation scheme [34], Chebyshev wavelet collocation method [34], Laguerre wavelet collocation approach [34], Bernoulli wavelet scheme [35–38], Haar wavelet method [39], Cardinal B-spline wavelet method [40].

Taylor wavelets are types of continuous wavelets. For the first time, Taylor wavelets were constructed in [41]. Numerous significant spaces are built on Taylor wavelets, which are small, spatially oriented oscillating functions. The given problem can be reduced to a collection of wavelet-based algebraic equations by estimating the integrals using operational matrices. This wavelet method has high accuracy and the ability to use quick algorithms. Compared to Chebyshev, Legendre, and Bernoulli wavelets, this method is simple and accurate and has low calculation costs [41]. Taylor wavelets produced by Taylor polynomials are a new accumulation to the field of wavelet families. The significance and advantages of the present work are as follows.

- Wavelets are mathematical functions that cut data into different frequency components and then study each component with a resolution matched to its scale.
- The number of terms of the Taylor polynomials $T_m(x)$ is less than the number of the Legendre and Fibonacci polynomials terms. It helps to reduce CPU time.
- The developed operational matrix of integration is sparse, resulting in a reduction in computing time.
- The Taylor wavelet is a function that may be defined at various scales and has a wide range of uses because of characteristics including compact support and vanishing moment.
- Some semi-analytical approaches depend on controlling parameters to work, but this TWM is controlling parameter-free.
- The proposed method is most suitable for studying solutions with discontinuity and sharp edges. We make a window for the function (at the point of discontinuity and sharp edges), and then we apply this method to get information about such functions.
- No obvious limitations of this strategy are apparent. But, this approach only works in a limited domain, not a broad one. We require the employment of transformations to operate throughout the vast domain.

Due to their superior properties and benefits, Taylor wavelets gathered the attention of many researchers toward them.

We found the following outstanding works about the Taylor wavelet technique in solving some of the equations throughout our review of the literature: Bratu-type equations [41], nonlinear fractional delay and pantograph differential equations [42], systems of nonlinear fractional differential equations [43], fractional delay differential equations [44], generalized Burgers-Huxley equation [45], fractional integrodifferential equations [46], Lane-Emden equations [47], Emden–Fowler equations [48], nonlinear coupled reaction–diffusion equation [49], fractional Volterra–Fredholm integrodifferential equations [50]. These are the recent developments on the Taylor wavelets.

According to the paragraph that follows, the article is structured. Section 2 covers the fractional derivative definition and the preliminaries of Taylor wavelets. Section 3 clarifies the function approximation of Taylor wavelets. Section 4 describes the functional integration matrix of Taylor wavelets. Section 5 explains the projected method of TWM. Section 6 denotes the applications of the present method. Finally, Sect. 7 covers the conclusion of the manuscript.

2 Preliminaries

2.1 Caputo fractional derivative

The Caputo fractional-order derivative of $f(t) \in C_\mu$ is defined by [51],

$$\frac{\partial^\delta f(t)}{\partial t^\delta} = \frac{1}{\Gamma(m-\delta)} \int_0^t (t-x)^{m-\delta-1} \frac{\partial^m f(x)}{\partial x^m} \mathrm{d}x,$$

for $m-1 < \delta \le m$, where $m = \lceil \delta \rceil$ be a positive integer, $t > 0$, $f(t) \in C_\mu^m$, $\mu \ge -1$.

2.2 Wavelets and Taylor wavelets

The family of functions known as wavelets are descended from a single function called the mother wavelet through dilatation and translation. When the translation parameter q and the dilation parameter p are continuously variable, we have the family of continuous wavelets shown in [27].

$$\lambda_{p,q}(r) = |p|^{-\frac{1}{2}} \lambda\left(\frac{r-q}{p}\right),\ p, q \in \mathbb{R},\ p \neq 0.$$

It introduces the discrete wavelet family as if $p = p_0^{-k}$, $q = nq_0p_0^{-k}$, $p_0 > 1$, $q_0 > 1$, and k and n are positive integers.

$$\lambda_{k,n}(r) = \left|p_0^{-k}\right|^{\frac{-1}{2}} \lambda\left(\frac{r - nq_0p_0^{-k}}{p_0^{-k}}\right) = |p_0|^{\frac{k}{2}} \lambda\left(p_0^k r - nq_0\right),$$

where $\lambda_{k,n}(r)$ is a wavelet basis for $L^2(\mathbb{R})$.

Taylor wavelets $\lambda_{n,m}(r) = \lambda(k, n, m, r)$ involve four arguments; $n = 1, 2, \ldots, 2^{k-1}$, m is the degree of Taylor polynomials, r is the normalized time, and k is any positive integer. On the interval $[0, 1)$, Taylor wavelets are defined as [42–44],

$$\lambda_{n,m}(r) = \begin{cases} 2^{\frac{k-1}{2}} \tilde{T}_m\left(2^{k-1}r - n + 1\right), & \frac{n-1}{2^{k-1}} \le r < \frac{n}{2^{k-1}}, \\ 0 & \text{Otherwise,} \end{cases}$$

with

$$\tilde{T}_m(r) = \sqrt{2m+1}\, T_m(r),$$

where $n = 1, 2, \ldots, 2^{k-1}$ and $m = 0, 1, 2, \ldots, M-1$. The coefficient $\sqrt{2m+1}$ is for normality, the dilation parameter is $p = 2^{-(k-1)}$ and the translation parameter $q = (n-1)2^{-(k-1)}$. $T_m(r)$ is the Taylor polynomial of degree m and it can be expressed as $T_m(r) = r^m$. Here, $\widetilde{T}_m(r)$ is the normal Taylor polynomial of degree m.

3 Function approximation

The Taylor wavelets can be used to expand a function $f(r) \in L^2[0, 1]$ as follows:

$$f(r) = \sum_{n=1}^{\infty} \sum_{m=0}^{\infty} c_{n,m} \lambda_{n,m}(r).$$

The above infinite series can be truncated to finite series for $f(r)$ as

$$f(r) = \sum_{n=1}^{2^{k-1}} \sum_{m=0}^{M-1} c_{n,m} \lambda_{n,m}(r) = A^T \lambda(r),$$

where T denotes the transposition and $A, \lambda(r)$ are $2^{k-1}M \times 1$ matrices given by

$$A^T = \left[c_{1,0}, \ldots, c_{1,M-1}, c_{2,0}, \ldots, c_{2,M-1}, \ldots, c_{2^{k-1},0}, \ldots c_{2^{k-1},M-1}\right],$$

$$\lambda(r) = \left[\lambda_{1,0}(r), \ldots, \lambda_{1,M-1}(r), \lambda_{2,0}(r), \ldots \lambda_{2,M-1}(r), \ldots \lambda_{2^{k-1},0}(r), \ldots \lambda_{2^{k-1},M-1}(r)\right]^T.$$

Let $\{\lambda_{n,m}\}$ is a sequence of Taylor wavelets, $m = 0, 1, \ldots,$ and $n = 1, 2, \ldots$. The components of the sequence $\{\lambda_{n,m}\}$ span a Taylor space for every fixed n.Hence $L(\{\lambda_{n,m}\}) = L^2[0, 1]$ becomes Banach space.

Theorem 1 *Let $X(r,\ t)$ in $L^2(\mathbb{R}\times\mathbb{R})$ is a continuous bounded function defined on $[0,\ 1]\times[0,\ 1]$, then Taylor wavelet expansion of $X(r,\ t)$ is uniformly converges to it.*

Proof Let $X(r,\ t)$ in $L^2(\mathbb{R}\times\mathbb{R})$ be a continuous function defined on $[0,\ 1]\times[0,\ 1]$ and bounded by a real number μ.The approximation of $X(r,\ t)$ is;

$$X(r,\ t)=\sum_{i=1}^{\infty}\sum_{j=0}^{\infty}a_{i,\ j}\lambda_{i,\ j}(r)\lambda_{i,\ j}(t),$$

where $a_{i,\ j}=\langle X(r,\ t),\ \lambda_{i,\ j}(r)\lambda_{i,\ j}(t)\rangle$, and $\langle,\ \rangle$ represents inner product.Since $\lambda_{i,\ j}(r)\lambda_{i,\ j}(t)$ are functions on $[0,\ 1]$.Then,

$$a_{i,\ j}=\int_0^1\int_0^1 X(r,\ t)\lambda_{i,\ j}(r)\lambda_{i,\ j}(t)\mathrm{d}r\mathrm{d}t,$$

$$a_{i,\ j}=\int_0^1\int_I X(r,\ t)2^{\frac{k-1}{2}}\sqrt{2m+1}T_m\Big(2^{k-1}r-n+1\Big)\lambda_{i,\ j}(t)\mathrm{d}r\mathrm{d}t,$$

where $I=\left[\frac{n-1}{2^{k-1}},\ \frac{n}{2^{k-1}}\right]$.Put $2^{k-1}r-n+1=x$ then,

$$a_{i,\ j}=2^{\frac{k-1}{2}}\sqrt{2m+1}\int_0^1\int_0^1 X\left(\frac{x-1+n}{2^{k-1}},\ t\right)T_m(x)\frac{\mathrm{d}x}{2^{k-1}}\lambda_{i,\ j}(t)\mathrm{d}t,$$

$$a_{i,\ j}=2^{-\left(\frac{k-1}{2}\right)}\sqrt{2m+1}\int_0^1\left[\int_0^1 X\left(\frac{x-1+n}{2^{k-1}},\ t\right)T_m(x)\mathrm{d}x\right]\lambda_{i,\ j}(t)\mathrm{d}t,$$

By using the generalized mean value theorem for integrals,

$$a_{i,\ j}=2^{-\left(\frac{k-1}{2}\right)}\sqrt{2m+1}\int_0^1 X\left(\frac{\xi-1+n}{2^{k-1}},\ t\right)\lambda_{i,\ j}(t)\mathrm{d}t\left[\int_0^1 T_m(x)\mathrm{d}x\right],$$

where $\xi\in(0,\ 1)$ and choose $\int_0^1 T_m(x)dx=A$,

$$a_{i,\ j}=A2^{-\left(\frac{k-1}{2}\right)}\sqrt{2m+1}\int_{\frac{n-1}{2^{k-1}}}^{\frac{n}{2^{k-1}}} X\left(\frac{\xi-1+n}{2^{k-1}},\ t\right)2^{\frac{k-1}{2}}\sqrt{2m+1}T_m\Big(2^{k-1}t-n+1\Big)\mathrm{d}t,$$

$$a_{i,\ j}=A(2m+1)\int_{\frac{n-1}{2^{k-1}}}^{\frac{n}{2^{k-1}}} X\Big(\tfrac{\xi-1+n}{2^{k-1}},\ t\Big)T_m\big(2^{k-1}t-n+1\big)\mathrm{d}t,$$

Put $2^{k-1}t-n+1=s$ then,

$$a_{i,\ j}=A(2m+1)\int_0^1 X\left(\frac{\xi-1+n}{2^{k-1}},\ \frac{s-1+n}{2^{k-1}}\right)T_m(s)\frac{\mathrm{d}s}{2^{k-1}},$$

$$a_{i,\ j}=A(2m+1)2^{-k+1}\int_0^1 X\Big(\tfrac{\xi-1+n}{2^{k-1}},\ \tfrac{s-1+n}{2^{k-1}}\Big)T_m(s)\mathrm{d}s,$$

Again, using the generalized mean value theorem for integrals,

$$a_{i,\ j}=A2^{-k+1}X\left(\frac{\xi-1+n}{2^{k-1}},\ \frac{\xi_1-1+n}{2^{k-1}}\right)\int_0^1 P_m(s)\mathrm{d}s,$$

where $\xi_1\in(0,\ 1)$ and $\int_0^1 P_m(s)ds=B$ then

$$a_{i,\ j}=AB\,(2m+1)\,2^{-k+1}X\left(\frac{\xi-1+n}{2^{k-1}},\ \frac{\xi_1-1+n}{2^{k-1}}\right),\quad\forall\xi,\ \xi_1\in(0,\ 1)$$

So,

$$\left|a_{i,\ j}\right|=\left|AB(2m+1)2^{-k+1}\right|\left|X\left(\frac{\xi-1+n}{2^{k-1}},\ \frac{\xi_1-1+n}{2^{k-1}}\right)\right|,$$

Since X is bounded by μ,

$$\left|a_{i,\ j}\right|=|A||B||2m+1|\left|2^{-k+1}\right|\mu.$$

Hence $\sum_{i=1}^{\infty}\sum_{j=0}^{\infty}a_{i,\ j}$ is convergent.Therefore, the Taylor wavelet expansion of $X(r,\ t)$ converges uniformly.

Theorem 2 [27] *Let the Taylor wavelet sequence $\{\lambda_{n,m}^k(t)\}_{k=1}^{\infty}$ which are continuous functions defined in $L^2(\mathbb{R})$ in t on $[a,\ b]$ converges to the function $\lambda(t)$ in $L^2(\mathbb{R})$ uniformly in t on $[a,\ b]$. Then $\lambda(t)$ is continuous in $L^2(\mathbb{R})$ in t on $[a,\ b]$.*

Theorem 3 [27] *Let the Taylor wavelet sequence $\{\lambda_{n,m}^k(t)\}_{k=1}^{\infty}$ converges itself in $L^2(\mathbb{R})$ uniformly in t on $[a,\ b]$. Then, there is a function $\lambda(t)$ that is continuous in $L^2(\mathbb{R})$ in t on $[a,\ b]$ and $lim_{k\to\infty}\lambda_{n,m}^k(t)=\lambda(t)\forall t\in[a,\ b]$.*

Theorem 4 [28] *Let $\{r_i=t_i/i=1,\ 2,\ \ldots,\ 2^{k-1}M^2\}$ be any set of $\frac{2i-1}{2^kM^2}$ distinct points in $[a,\ b]$ and $X(r,\ t)\in c[a,\ b]$, where $c[a,\ b]$ is a set of all continuous functions defined in $[a,\ b]$. $X(r,\ t)$ be the solution of the given partial differential equation; then there is exactly one linear combination $\Phi(r,\ t)$ of polynomial-based wavelet functions that satisfy the.*

$$X(r_i,\ t_i)=\Phi(r_i,\ t_i)\ \forall i=1,\ 2,\ \ldots,\ 2^{k-1}M^2.$$

4 Operational matrix of integration

At $k = 1$ and $M = 6$, the Taylor wavelet basis is obtained as below:

$$\lambda_{1,0}(r) = 1,$$

$$\lambda_{1,1}(r) = \sqrt{3}r,$$

$$\lambda_{1,2}(r) = \sqrt{5}r^2,$$

$$\lambda_{1,3}(r) = \sqrt{7}r^3,$$

$$\lambda_{1,4}(r) = 3r^4,$$

$$\lambda_{1,5}(r) = \sqrt{11}r^5,$$

$$\lambda_{1,6}(r) = \sqrt{13}r^6,$$

$$\lambda_{1,7}(r) = \sqrt{15}r^7.$$

Integrating the above basis concerning r limit from 0 to r, the Taylor wavelet bases are then expressed as a linear combination as:

$$\int_0^r \lambda_{1,0}(r)\mathrm{d}r = \left[\begin{array}{ccccc} 0 & \frac{1}{\sqrt{3}} & 0 & 0 & 0 \end{array}\right]\lambda_6(r),$$

$$\int_0^r \lambda_{1,1}(r)\mathrm{d}r = \left[\begin{array}{ccccc} 0 & 0 & \frac{\sqrt{3}}{2\sqrt{5}} & 0 & 0 \end{array}\right]\lambda_6(r),$$

$$\int_0^r \lambda_{1,2}(r)\mathrm{d}r = \left[\begin{array}{ccccc} 0 & 0 & 0 & \frac{\sqrt{5}}{3\sqrt{7}} & 0 \end{array}\right]\lambda_6(r),$$

$$\int_0^r \lambda_{1,3}(r)\mathrm{d}r = \left[\begin{array}{ccccc} 0 & 0 & 0 & 0 & \frac{\sqrt{7}}{12} \end{array}\right]\lambda_6(r),$$

$$\int_0^r \lambda_{1,4}(r)\mathrm{d}r = \left[\begin{array}{ccccc} 0 & 0 & 0 & 0 & 0 \end{array}\right]\lambda_6(r),$$

$$\int_0^r \lambda_{1,5}(r)\mathrm{d}r = \left[\begin{array}{cccccc} 0 & 0 & 0 & 0 & 0 & 0 \end{array}\right]\lambda_6(r) + \frac{\sqrt{11}}{6\sqrt{13}}\lambda_{1,6}(r).$$

And

$$\lambda_6(r) = \left[\lambda_{1,0}(r),\ \lambda_{1,1}(r),\ \lambda_{1,2}(r),\ \lambda_{1,3}(r),\ \lambda_{1,4}(r),\ \lambda_{1,5}(r)\right]^T.$$

Hence,

$$\int_0^r \lambda(r)\mathrm{d}r = \mathbb{B}_{6\times 6}\lambda_6(r) + \overline{\lambda_6(r)}, \tag{4.1}$$

where

$$\mathbb{B}_{6\times 6} = \begin{bmatrix} 0 & \frac{1}{\sqrt{3}} & 0 & 0 & 0 & 0 \\ 0 & 0 & \frac{\sqrt{3}}{2\sqrt{5}} & 0 & 0 & 0 \\ 0 & 0 & 0 & \frac{\sqrt{5}}{3\sqrt{7}} & 0 & 0 \\ 0 & 0 & 0 & 0 & \frac{\sqrt{7}}{12} & 0 \\ 0 & 0 & 0 & 0 & 0 & \frac{3}{5\sqrt{11}} \\ 0 & 0 & 0 & 0 & 0 & 0 \end{bmatrix} \text{ and } \overline{\lambda_6(r)} = \begin{bmatrix} 0 \\ 0 \\ 0 \\ 0 \\ 0 \\ \frac{\sqrt{11}}{6\sqrt{13}}\lambda_{1,6}(r) \end{bmatrix}.$$

The generalized first integration of n-wavelet basis at $k = 1$ is defined as:

$$\int_0^r \lambda(r)\mathrm{d}r = \mathbb{B}_{n\times n}\lambda(r) + \overline{\lambda_n(r)},$$

where

$$\mathbb{B}_{n\times n} = \begin{bmatrix} 0 & \frac{1}{\sqrt{3}} & 0 & 0 & 0 & \cdots & 0 & 0 \\ 0 & 0 & \frac{\sqrt{3}}{2\sqrt{5}} & 0 & 0 & \cdots & 0 & 0 \\ 0 & 0 & 0 & \frac{\sqrt{5}}{3\sqrt{7}} & 0 & \cdots & 0 & 0 \\ 0 & 0 & 0 & 0 & \frac{\sqrt{7}}{12} & \cdots & 0 & 0 \\ \vdots & \vdots & \vdots & \vdots & \ddots & \ddots & 0 & 0 \\ 0 & 0 & 0 & 0 & 0 & 0 & \frac{\sqrt{2(n-2)+1}}{(n-1)\sqrt{2(n-2)+3}} & 0 \\ 0 & 0 & 0 & 0 & 0 & \cdots & 0 & \frac{\sqrt{2(n-1)+1}}{n\sqrt{2(n-1)+3}} \\ 0 & 0 & 0 & 0 & 0 & \cdots & 0 & 0 \end{bmatrix} \text{ and}$$

$$\overline{\lambda_n(r)} = \begin{bmatrix} 0 \\ 0 \\ 0 \\ 0 \\ 0 \\ 0 \\ \vdots \\ \frac{\sqrt{2n-1}}{n\sqrt{2n+1}}\lambda_{1,n}(r) \end{bmatrix}.$$

Integrating the basis once again, we attain the following;

$$\int_0^r\int_0^r \lambda_{1,0}(r)\mathrm{d}r = \left[\begin{array}{ccccc} 0 & 0 & \frac{1}{2\sqrt{5}} & 0 & 0 \end{array}\right]\lambda_6(r),$$

$$\int_0^r\int_0^r \lambda_{1,1}(r)dr = \left[\begin{array}{ccccc} 0 & 0 & 0 & \frac{1}{2\sqrt{21}} & 0 \end{array}\right]\lambda_6(r),$$

$$\int_0^r\int_0^r \lambda_{1,2}(r)dr = \left[\begin{array}{ccccc} 0 & 0 & 0 & 0 & \frac{\sqrt{5}}{36} \end{array}\right]\lambda_6(r),$$

$$\int_0^r\int_0^r \lambda_{1,3}(r)\mathrm{d}r = \left[\begin{array}{cccccc} 0 & 0 & 0 & 0 & 0 & \frac{\sqrt{7}}{20\sqrt{11}} \end{array}\right]\lambda_6(r),$$

$$\int_0^r\int_0^r \lambda_{1,4}(r)\mathrm{d}r = \left[\begin{array}{cccccc} 0 & 0 & 0 & 0 & 0 & 0 \end{array}\right]\lambda_6(r) + \frac{1}{10\sqrt{13}}\lambda_{1,6}(r),$$

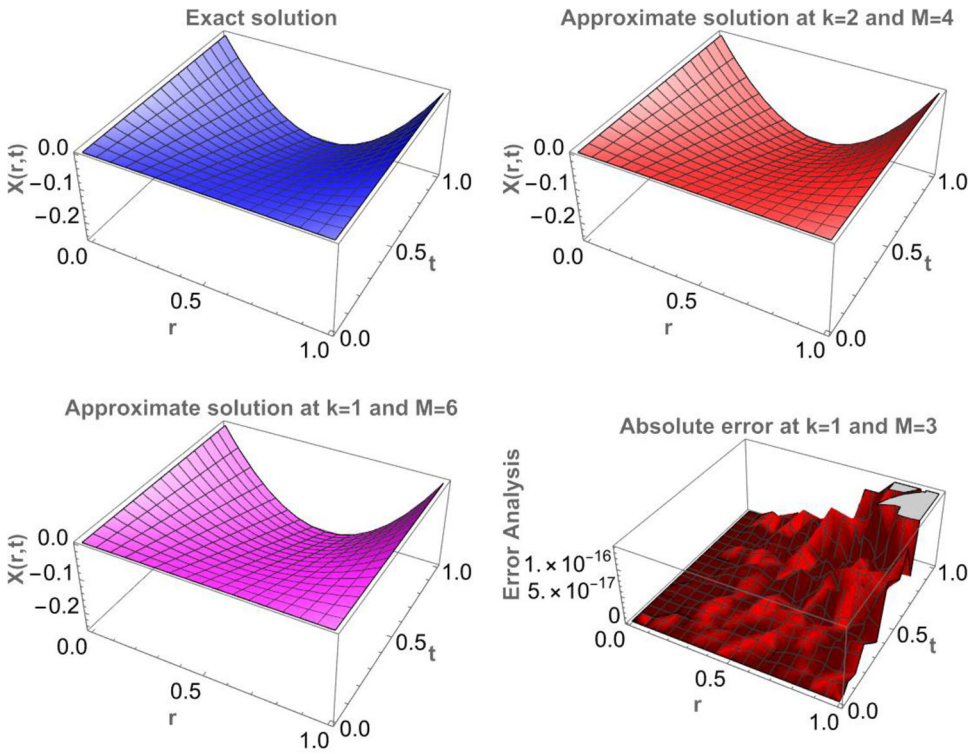

Fig. 1 The exact solution, approximate solution for different values of k and M, and an absolute error, for example, 6.1

$$\int_0^r \int_0^r \lambda_{1,5}(r)dr = \begin{bmatrix} 0\ 0\ 0\ 0\ 0\ 0 \end{bmatrix}\lambda_6(r) + \frac{\sqrt{11}}{42\sqrt{15}}\lambda_{1,7}(r).$$

Hence,

$$\int_0^r \int_0^r \lambda(r)\mathrm{d}r = \mathbb{B}'_{6\times 6}\lambda_6(r) + \overline{\lambda'_6(r)}, \tag{4.2}$$

where

$$\mathbb{B}'_{6\times 6} = \begin{bmatrix} 0\ 0 & \frac{1}{2\sqrt{5}} & 0 & 0 & 0 \\ 0\ 0 & 0 & \frac{1}{2\sqrt{21}} & 0 & 0 \\ 0\ 0 & 0 & 0 & \frac{\sqrt{5}}{36} & 0 \\ 0\ 0 & 0 & 0 & 0 & \frac{\sqrt{7}}{20\sqrt{11}} \\ 0\ 0 & 0 & 0 & 0 & 0 \\ 0\ 0 & 0 & 0 & 0 & 0 \end{bmatrix} \text{ and}$$

$$\overline{\lambda'_6(r)} = \begin{bmatrix} 0 \\ 0 \\ 0 \\ 0 \\ \frac{1}{10\sqrt{13}}\lambda_{1,6}(r) \\ \frac{\sqrt{11}}{42\sqrt{15}}\lambda_{1,7}(r) \end{bmatrix}.$$

The Taylor wavelet basis is examined at $k = 2$ and $M = 6$ as follows:

$$\left.\begin{array}{c} \lambda_{1,0}(r) = \sqrt{2} \\ \lambda_{1,1}(r) = 2\sqrt{6}r \\ \lambda_{1,2}(r) = 4\sqrt{10}r^2 \\ \lambda_{1,3}(r) = 8\sqrt{14}r^3 \\ \lambda_{1,4}(r) = 48\sqrt{2}r^4 \\ \lambda_{1,5}(r) = 32\sqrt{22}r^5 \end{array}\right\} \quad 0 \le r < \frac{1}{2},$$

$$\left.\begin{array}{c} \lambda_{2,0}(r) = \sqrt{2} \\ \lambda_{2,1}(r) = \sqrt{6}(-1+2r) \\ \lambda_{2,2}(r) = \sqrt{10}(1-2r)^2 \\ \lambda_{2,3}(r) = \sqrt{14}(-1+2r)^3 \\ \lambda_{2,4}(r) = 3\sqrt{2}(1-2r)^4 \\ \lambda_{2,5}(r) = \sqrt{22}(-1+2r)^5 \end{array}\right\} \quad \frac{1}{2} \le r < 1.$$

Integrating the above basis concerning r limit from 0 to r, the Taylor wavelet bases are then expressed as a linear combination as:

$$\int_0^r \lambda(r)\mathrm{d}r = \mathbb{B}_{12\times 12}\lambda_{12}(r) + \overline{\lambda_{12}(r)}, \tag{4.3}$$

where

$$\lambda_{12}(r) = [\lambda_{1,0}(r),\ \lambda_{1,1}(r),\ \lambda_{1,2}(r),\ \lambda_{1,3}(r),\ \lambda_{1,4}(r),\ \lambda_{1,5}(r),\ \lambda_{2,0}(r),\ \lambda_{2,1}(r),\ \lambda_{2,2}(r),\ \lambda_{2,3}(r),\ \lambda_{2,4}(r),\ \lambda_{2,5}(r)]^T.$$

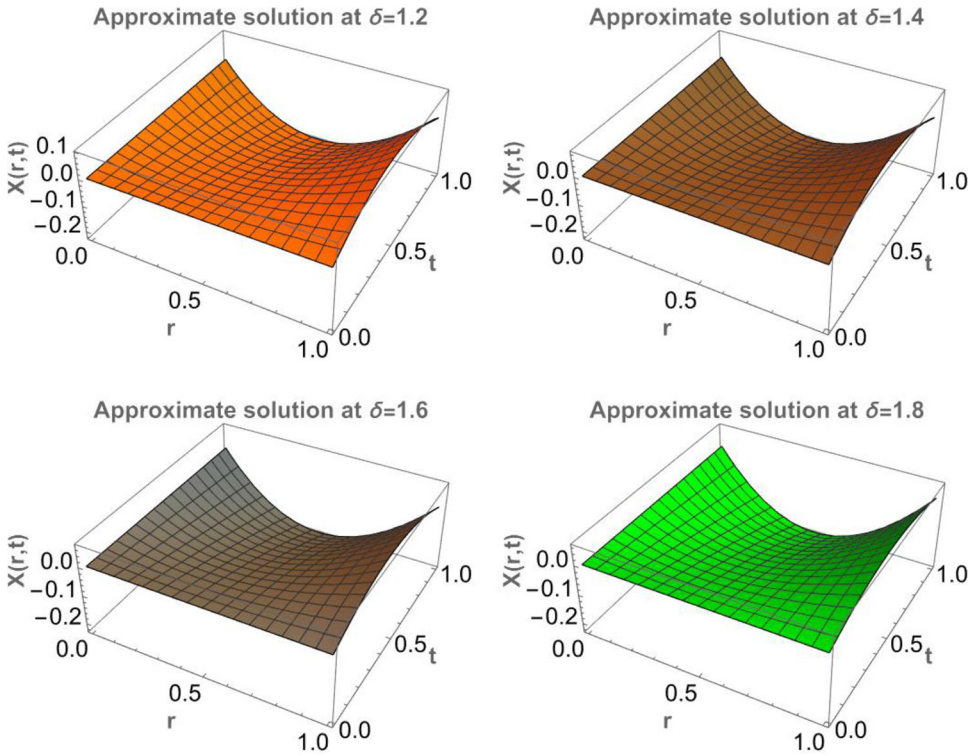

Fig. 2 Present method solution at $k = 1$, $M = 7$, and different values of δ, for example, 6.1

Table 1 The present method solution for $r = 0.1$, $k = 1$, $M = 4$, and at different values of δ, for example, 6.1. (CPU time: 0.582 sec)

t	TWM				
	$\delta = 1.1$	$\delta = 1.3$	$\delta = 1.5$	$\delta = 1.7$	$\delta = 1.9$
0.1	−0.00853383	−0.00853255	−0.00853402	−0.00854092	−0.00855599
0.2	−0.01712786	−0.01712588	−0.01713031	−0.01714612	−0.01717690
0.3	−0.02578208	−0.02578000	−0.02578887	−0.02581560	−0.02586270
0.4	−0.03449651	−0.03449489	−0.03450969	−0.03454935	−0.03461342
0.5	−0.04327113	−0.04327058	−0.04329278	−0.04334738	−0.04342904
0.6	−0.05210594	−0.05210704	−0.05213813	−0.05220969	−0.05230956
0.7	−0.06100096	−0.06100429	−0.06104575	−0.06113628	−0.06125499
0.8	−0.06995617	−0.06996232	−0.07001563	−0.07012714	−0.07026533
0.9	−0.07897157	−0.07898113	−0.07904778	−0.07918228	−0.07934057

$$\mathbb{B}_{12\times 12} = \begin{bmatrix} 0 & \frac{1}{2\sqrt{3}} & 0 & 0 & 0 & 0 & 0 & 0 & 0 & 0 & 0 & 0 \\ 0 & 0 & \frac{\sqrt{\frac{3}{5}}}{4} & 0 & 0 & 0 & 0 & 0 & 0 & 0 & 0 & 0 \\ 0 & 0 & 0 & \frac{\sqrt{\frac{5}{7}}}{6} & 0 & 0 & 0 & 0 & 0 & 0 & 0 & 0 \\ 0 & 0 & 0 & 0 & \frac{\sqrt{7}}{24} & 0 & 0 & 0 & 0 & 0 & 0 & 0 \\ 0 & 0 & 0 & 0 & 0 & \frac{3}{10\sqrt{11}} & 0 & 0 & 0 & 0 & 0 & 0 \\ 0 & 0 & 0 & 0 & 0 & 0 & 0 & 0 & 0 & 0 & 0 & 0 \\ 0 & 0 & 0 & 0 & 0 & 0 & 0 & \frac{1}{2\sqrt{3}} & 0 & 0 & 0 & 0 \\ 0 & 0 & 0 & 0 & 0 & 0 & 0 & 0 & \frac{\sqrt{\frac{3}{5}}}{4} & 0 & 0 & 0 \\ 0 & 0 & 0 & 0 & 0 & 0 & 0 & 0 & 0 & \frac{\sqrt{\frac{5}{7}}}{6} & 0 & 0 \\ 0 & 0 & 0 & 0 & 0 & 0 & 0 & 0 & 0 & 0 & \frac{\sqrt{7}}{24} & 0 \\ 0 & 0 & 0 & 0 & 0 & 0 & 0 & 0 & 0 & 0 & 0 & \frac{3}{10\sqrt{11}} \\ 0 & 0 & 0 & 0 & 0 & 0 & 0 & 0 & 0 & 0 & 0 & 0 \end{bmatrix} \text{ and } \quad \overline{\lambda_{12}(r)} = \begin{bmatrix} 0 \\ 0 \\ 0 \\ 0 \\ 0 \\ \frac{\sqrt{\frac{11}{13}}}{12}\lambda_{1,6}(r) \\ 0 \\ 0 \\ 0 \\ 0 \\ 0 \\ \frac{\sqrt{\frac{11}{13}}}{12}\lambda_{2,6}(r) \end{bmatrix}.$$

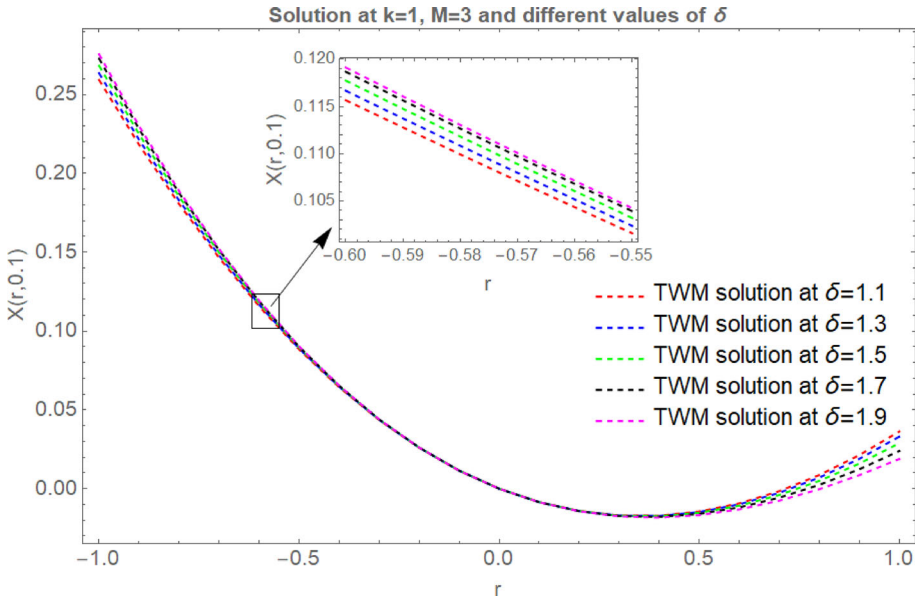

Fig. 3 Present method solution at $t = 0.1$ and different values of δ, for example, 6.1

The generalized first integration of n-wavelet basis at $k = 2$ is defined as:

where

$$\int_0^r \lambda(r)dr = \mathbb{B}_{2n\times 2n}\lambda(r) + \overline{\lambda_{2n}(r)},$$

$$\mathbb{B}_{2n\times 2n} = \begin{bmatrix}
0 & \frac{1}{2\sqrt{3}} & 0 & 0 & 0 & \cdots & 0 & 0 & 0 & 0 & 0 & 0 & 0 & 0 & 0 & 0 \\
0 & 0 & \frac{\sqrt{\frac{3}{5}}}{4} & 0 & 0 & \cdots & 0 & 0 & 0 & 0 & 0 & 0 & 0 & 0 & 0 & 0 \\
0 & 0 & 0 & \frac{\sqrt{\frac{5}{7}}}{6} & 0 & \cdots & 0 & 0 & 0 & 0 & 0 & 0 & 0 & 0 & 0 & 0 \\
0 & 0 & 0 & 0 & \frac{\sqrt{7}}{24} & \cdots & 0 & 0 & 0 & 0 & 0 & 0 & 0 & 0 & 0 & 0 \\
\vdots & \vdots & \vdots & \vdots & \ddots & \ddots & 0 & 0 & 0 & 0 & 0 & 0 & 0 & 0 & 0 & 0 \\
0 & 0 & 0 & 0 & 0 & 0 & \frac{\sqrt{2(n-2)+1}}{(2n-1)\sqrt{2(n-2)+3}} & 0 & 0 & 0 & 0 & 0 & 0 & 0 & 0 & 0 \\
0 & 0 & 0 & 0 & 0 & 0 & 0 & \frac{\sqrt{2(n-1)+1}}{2n\sqrt{2(n-1)+3}} & 0 & 0 & 0 & 0 & 0 & 0 & 0 & 0 \\
0 & 0 & 0 & 0 & 0 & 0 & 0 & 0 & 0 & 0 & 0 & 0 & 0 & 0 & 0 & 0 \\
0 & 0 & 0 & 0 & 0 & 0 & 0 & 0 & 0 & \frac{1}{2\sqrt{3}} & 0 & 0 & 0 & \ldots & 0 & 0 \\
0 & 0 & 0 & 0 & 0 & 0 & 0 & 0 & 0 & 0 & \frac{\sqrt{\frac{3}{5}}}{4} & 0 & 0 & \ldots & 0 & 0 \\
0 & 0 & 0 & 0 & 0 & 0 & 0 & 0 & 0 & 0 & 0 & \frac{\sqrt{\frac{5}{7}}}{6} & 0 & \ldots & 0 & 0 \\
0 & 0 & 0 & 0 & 0 & 0 & 0 & 0 & 0 & 0 & 0 & 0 & \frac{\sqrt{7}}{24} & \ldots & 0 & 0 \\
0 & 0 & 0 & 0 & 0 & 0 & 0 & 0 & \vdots & \vdots & \vdots & \vdots & \ddots & \ddots & \frac{\sqrt{2(n-2)+1}}{(2n-1)\sqrt{2(n-2)+3}} & 0 \\
0 & 0 & 0 & 0 & 0 & 0 & 0 & 0 & 0 & 0 & 0 & 0 & 0 & 0 & 0 & \frac{\sqrt{2(n-1)+1}}{2n\sqrt{2(n-1)+3}} \\
0 & 0 & 0 & 0 & 0 & 0 & 0 & 0 & 0 & 0 & 0 & 0 & 0 & 0 & 0 & 0
\end{bmatrix}$$

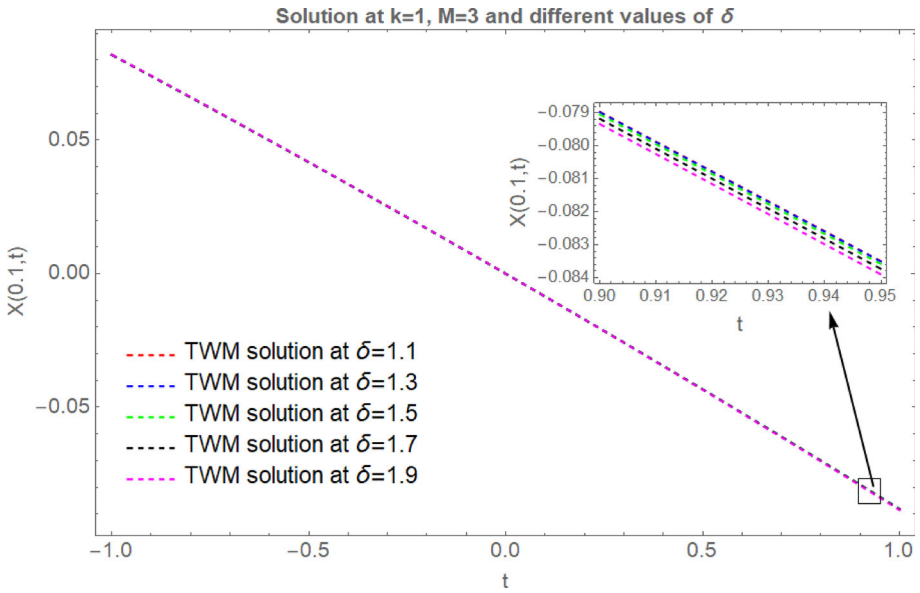

Fig. 4 Present method solution at $r = 0.1$ and different values of δ, for example, 6.1

$$\text{and } \overline{\lambda_{2n}(r)} = \begin{bmatrix} 0 \\ 0 \\ 0 \\ 0 \\ 0 \\ \vdots \\ \frac{\sqrt{2n-1}}{2n\sqrt{2n+1}}\lambda_{1,n}(r) \\ 0 \\ 0 \\ 0 \\ 0 \\ 0 \\ \vdots \\ \frac{\sqrt{2n-1}}{2n\sqrt{2n+1}}\lambda_{2,n}(r) \end{bmatrix}.$$

Similarly, the second integration can be written as:

$$\int_0^r \int_0^r \lambda(r)\mathrm{d}r\mathrm{d}r = \mathbb{B}'_{12\times 12}\lambda_{12}(r) + \overline{\lambda'_{12}(r)}, \tag{4.4}$$

where

$$\lambda_{12}(r) = \big[\lambda_{1,0}(r),\ \lambda_{1,1}(r),\ \lambda_{1,2}(r),\ \lambda_{1,3}(r),\ \lambda_{1,4}(r),\ \lambda_{1,5}(r),\ \lambda_{2,0}(r),\ \lambda_{2,1}(r),\ \lambda_{2,2}(r),\ \lambda_{2,3}(r),\ \lambda_{2,4}(r),\ \lambda_{2,5}(r)\big]^T.$$

$$\mathbb{B}'_{12\times 12} = \begin{bmatrix} 0 & 0 & \frac{1}{8\sqrt{5}} & 0 & 0 & 0 & 0 & 0 & 0 & 0 & 0 & 0 \\ 0 & 0 & 0 & \frac{1}{8\sqrt{21}} & 0 & 0 & 0 & 0 & 0 & 0 & 0 & 0 \\ 0 & 0 & 0 & 0 & \frac{\sqrt{5}}{144} & 0 & 0 & 0 & 0 & 0 & 0 & 0 \\ 0 & 0 & 0 & 0 & 0 & \frac{\sqrt{\frac{7}{11}}}{80} & 0 & 0 & 0 & 0 & 0 & 0 \\ 0 & 0 & 0 & 0 & 0 & 0 & 0 & 0 & 0 & 0 & 0 & 0 \\ 0 & 0 & 0 & 0 & 0 & 0 & 0 & 0 & 0 & 0 & 0 & 0 \\ 0 & 0 & 0 & 0 & 0 & 0 & 0 & \frac{1}{8\sqrt{5}} & 0 & 0 & 0 & 0 \\ 0 & 0 & 0 & 0 & 0 & 0 & 0 & 0 & \frac{1}{8\sqrt{21}} & 0 & 0 & 0 \\ 0 & 0 & 0 & 0 & 0 & 0 & 0 & 0 & 0 & \frac{\sqrt{5}}{144} & 0 & 0 \\ 0 & 0 & 0 & 0 & 0 & 0 & 0 & 0 & 0 & 0 & \frac{\sqrt{\frac{7}{11}}}{80} & 0 \\ 0 & 0 & 0 & 0 & 0 & 0 & 0 & 0 & 0 & 0 & 0 & 0 \\ 0 & 0 & 0 & 0 & 0 & 0 & 0 & 0 & 0 & 0 & 0 & 0 \end{bmatrix} \text{ and}$$

$$\overline{\lambda'_{12}(r)} = \begin{bmatrix} 0 \\ 0 \\ 0 \\ 0 \\ \frac{1}{40\sqrt{13}}\lambda_{1,6}(r) \\ \frac{\sqrt{\frac{11}{15}}}{168}\lambda_{1,7}(r) \\ 0 \\ 0 \\ 0 \\ 0 \\ \frac{1}{40\sqrt{13}}\lambda_{2,6}(r) \\ \frac{\sqrt{\frac{11}{15}}}{168}\lambda_{2,7}(r) \end{bmatrix}.$$

Similarly, we can generate matrices for our convenience.

Table 2 The comparison of absolute errors of the projected method with different methods at different values of k, M, and $t = 1$, $\delta = 2$, for example, 6.1. (CPU time: 0.652 sec)

r	Taylor wavelet		Fibonacci wavelet [53]		Legendre wavelet [52]	Sinc-Legendre [54]
	$k = 1, M = 3$	$k = 2, M = 4$	$k = 2, M = 3$	$k = 2, M = 5$	$k = 2, M = 4$	$n = 3, m = 7$
0.1	1.7347×10^{-18}	8.6736×10^{-19}	8.3267×10^{-17}	1.0714×10^{-18}	1.3877×10^{-17}	1.6932×10^{-4}
0.2	0	1.7347×10^{-18}	2.2204×10^{-16}	2.2204×10^{-18}	2.7755×10^{-17}	1.0916×10^{-3}
0.3	6.9388×10^{-18}	0	4.2896×10^{-15}	2.1957×10^{-18}	5.5511×10^{-17}	1.0749×10^{-3}
0.4	0	1.7347×10^{-18}	2.7756×10^{-17}	1.5266×10^{-17}	2.7755×10^{-17}	1.0102×10^{-3}
0.5	6.9388×10^{-18}	0	2.7756×10^{-17}	2.4182×10^{-17}	2.7755×10^{-17}	9.9270×10^{-4}
0.6	1.3877×10^{-17}	1.7347×10^{-18}	2.7756×10^{-17}	1.9429×10^{-18}	8.3266×10^{-17}	1.0102×10^{-3}
0.7	1.7347×10^{-17}	5.2041×10^{-18}	1.3878×10^{-16}	1.8041×10^{-18}	8.3266×10^{-17}	1.0749×10^{-3}
0.8	3.4694×10^{-18}	0	1.3878×10^{-16}	2.5258×10^{-17}	5.5511×10^{-17}	1.0916×10^{-3}
0.9	1.2143×10^{-17}	6.0715×10^{-18}	9.7145×10^{-17}	4.1737×10^{-17}	5.5511×10^{-17}	7.6032×10^{-4}

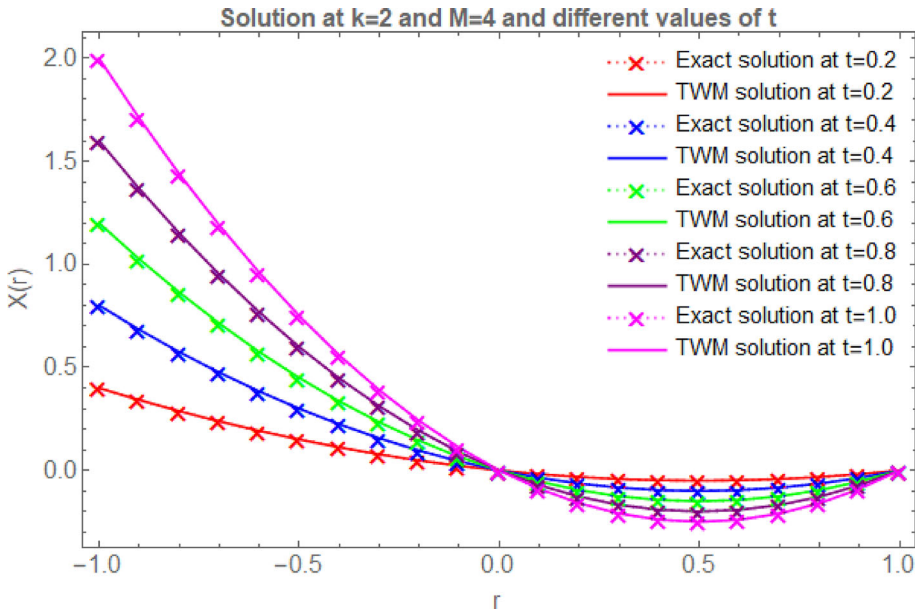

Fig. 5 Present method solution at different values of t, for example, 6.1

5 Method of solution

The primary goal of this part is to introduce a novel method based on Taylor wavelets for solving the telegraph equation. Consider the fractional PDE of the following type:

$$\frac{\partial^{\delta} X(r,\, t)}{\partial t^{\delta}} + a\frac{\partial^{\delta-1} X(r,\, t)}{\partial t^{\delta-1}} + bX(r,\, t) = c\frac{\partial^2 X(r,\, t)}{\partial r^2} + h(r,\, t), \tag{5.1}$$

where r, t are the independent variables and X is a dependent variable with the given physical conditions.

$$X(r,\, 0) = L_1(r),\ X(0,\, t) = L_2(t),\ X(c,\, t) = L_3(t), \tag{5.2}$$

where c be any constant, $L_1(r)$, $L_2(t)$, and $L_3(t)$ are the real-valued and continuous functions. Let's assume,

$$\frac{\partial^3 X(r,\, t)}{\partial r^2 \partial t} \approx \lambda^T(r) Q \lambda(t). \tag{5.3}$$

where $\lambda^T(r) = \left[\lambda_{1,0}(r), \ldots, \lambda_{1,M-1}(r), \ldots, \lambda_{2^{k-1},0}(r), \ldots, \lambda_{2^{k-1},M-1}(r)\right]$,

$Q = \left[b_{i,j}\right]$ be $2^{k-1}M \times 2^{k-1}M$ unknown matrix such that $i,\ j = 1, \ldots, 2^{k-1}M$.

$$\lambda(t) = \left[\lambda_{1,0}(t),\ \ldots,\ \lambda_{1,M-1}(t),\ \ldots,\ \lambda_{2^{k-1},0}(t),\ \ldots,\ \lambda_{2^{k-1},M-1}(t)\right]^T,$$

By integrating Eq. (5.3) concerning to t from limit 0 to t.

$$\frac{\partial^2 X(r,\, t)}{\partial r^2} = \frac{\partial^2 X(r,\, 0)}{\partial r^2} + \lambda^T(r) Q \left[\mathbb{B}\lambda(t) + \bar{\lambda}(t)\right], \tag{5.4}$$

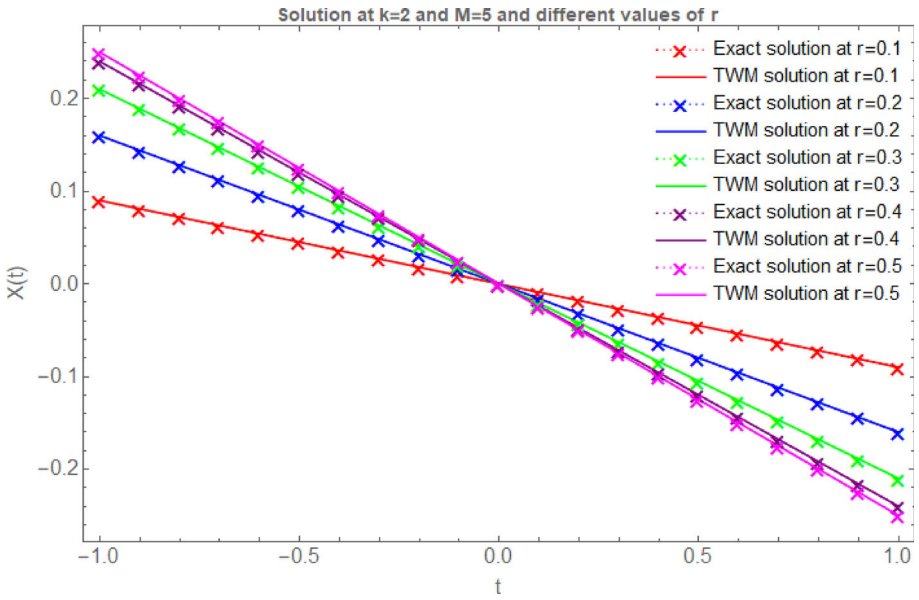

Fig. 6 Present method solution at different values of r, for example, 6.1

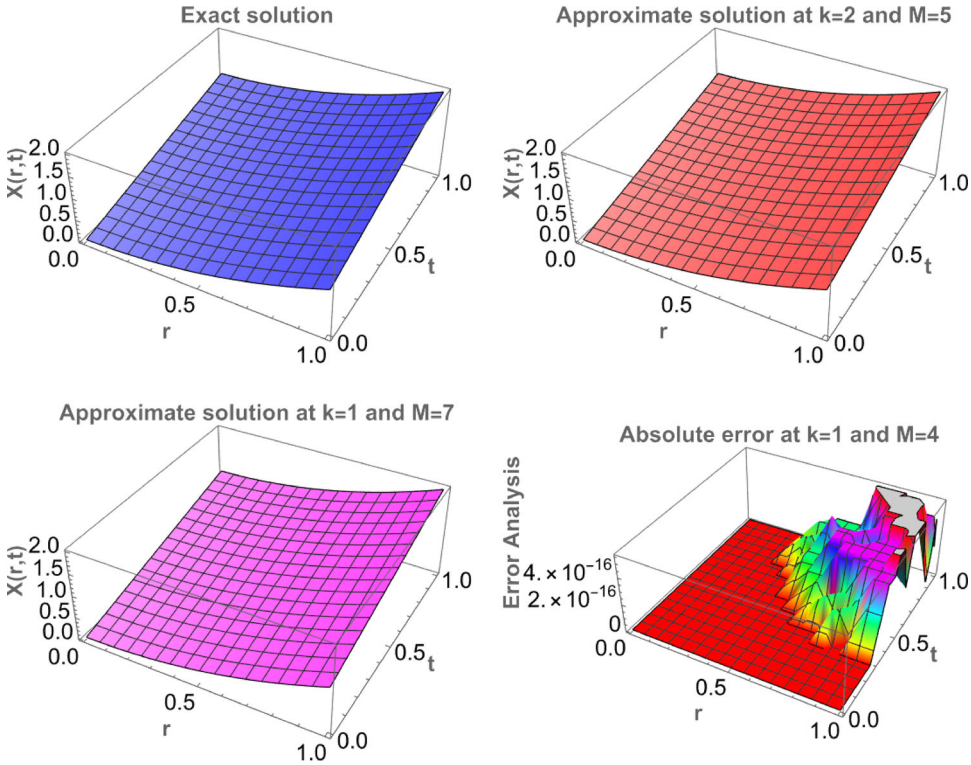

Fig. 7 The exact solution, approximate solution for different values of k and M, and an absolute error, for example, 6.2

Now integrate Eq. (5.4) twice concerning to r from 0 to r.

$$\frac{\partial X(r,t)}{\partial r} = \frac{\partial X(0,t)}{\partial r} + \frac{\partial X(r,0)}{\partial r} - \frac{\partial X(0,0)}{\partial r} + \left[\mathbb{B}\lambda(r) + \bar{\lambda}(r)\right]^T Q \left[\mathbb{B}\lambda(t) + \bar{\lambda}(t)\right], \tag{5.5}$$

$$X(r,t) = X(0,t) + X(r,0) - X(0,0) + r\left[\frac{\partial X(0,t)}{\partial r} - \frac{\partial X(0,0)}{\partial r}\right] + \left[\mathbb{B}\lambda(r) + \bar{\lambda}(r)\right]^{T} Q \left[\mathbb{B}\lambda(t) + \bar{\lambda}(t)\right], \tag{5.6}$$

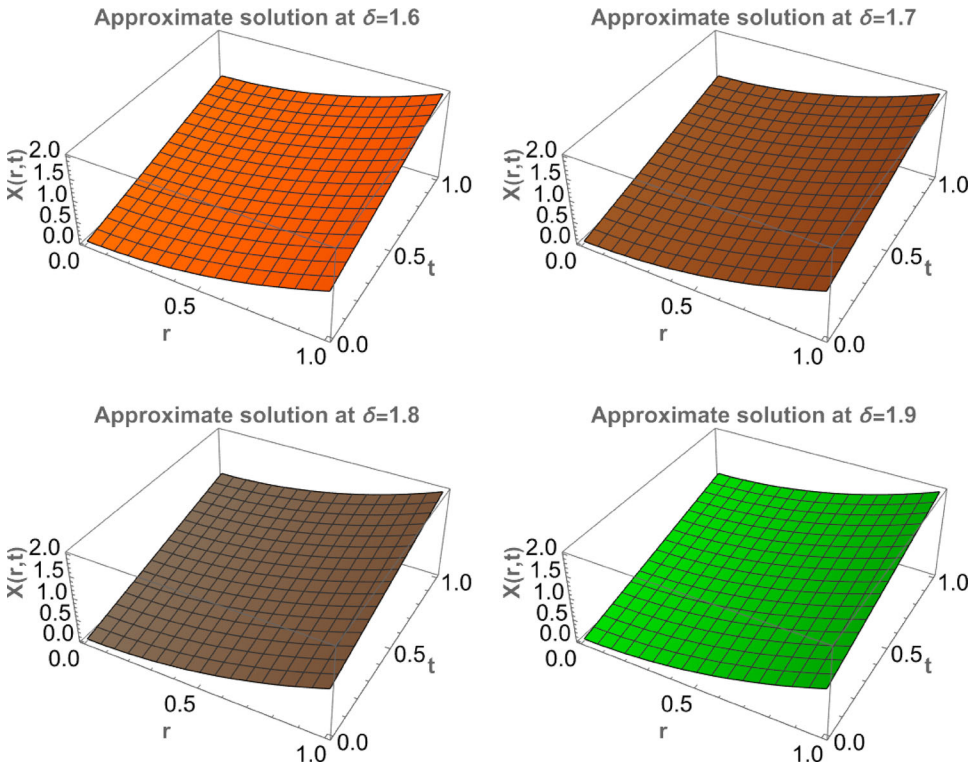

Fig. 8 Present method solution at $k = 2$, $M = 3$, and different values of δ, for example, 6.2

Table 3 The present method solution at $r = 0.1$, $k = 1$, $M = 4$, and for different values of δ, for example, 6.2. (CPU time: 0.571 sec)

t	TWM				
	$\delta = 1.1$	$\delta = 1.3$	$\delta = 1.5$	$\delta = 1.7$	$\delta = 1.9$
0.1	0.10077545	0.10086582	0.10099690	0.10121141	0.10152947
0.2	0.19243336	0.19286587	0.19332289	0.19386331	0.19445694
0.3	0.28497373	0.28600014	0.28697798	0.28795569	0.28878241
0.4	0.37839657	0.38026865	0.38196217	0.38348855	0.38450588
0.5	0.47270186	0.47567139	0.47827544	0.48046190	0.48162735
0.6	0.56788962	0.57220835	0.57591781	0.57887572	0.58014681
0.7	0.66395984	0.66987954	0.67488927	0.67873003	0.68006428
0.8	0.76091251	0.76868496	0.77518983	0.78002483	0.78137974
0.9	0.85874765	0.86862461	0.87681948	0.88276010	0.88409321

Put $r = c$ in Eq. (5.6) along with the given physical conditions in Eq. (5.2). We attain,

$$L_3(t) = L_2(t) + L_1(c) - L_1(0) + c\left[\frac{\partial X(0,t)}{\partial r} - \frac{\partial X(0,0)}{\partial r}\right] + \lim_{r\to c}\left[\mathbb{B}\prime\lambda(r) + \bar{\lambda}(r)'\right]^T Q\left[\mathbb{B}\lambda(t) + \bar{\lambda}(t)\right],$$

$$\left[\frac{\partial X(0,t)}{\partial r} - \frac{\partial X(0,0)}{\partial r}\right] = \frac{1}{c}\left[L_3(t) - L_2(t) - L_1(c) + L_1(0) - \lim_{r\to c}\left[\mathbb{B}\prime\lambda(r) + \bar{\lambda}(r)'\right]^T Q\left[\mathbb{B}\lambda(t) + \bar{\lambda}(t)\right]\right], \tag{5.7}$$

Substitute Eq. (5.7) in Eqs. (5.5) and (5.6)

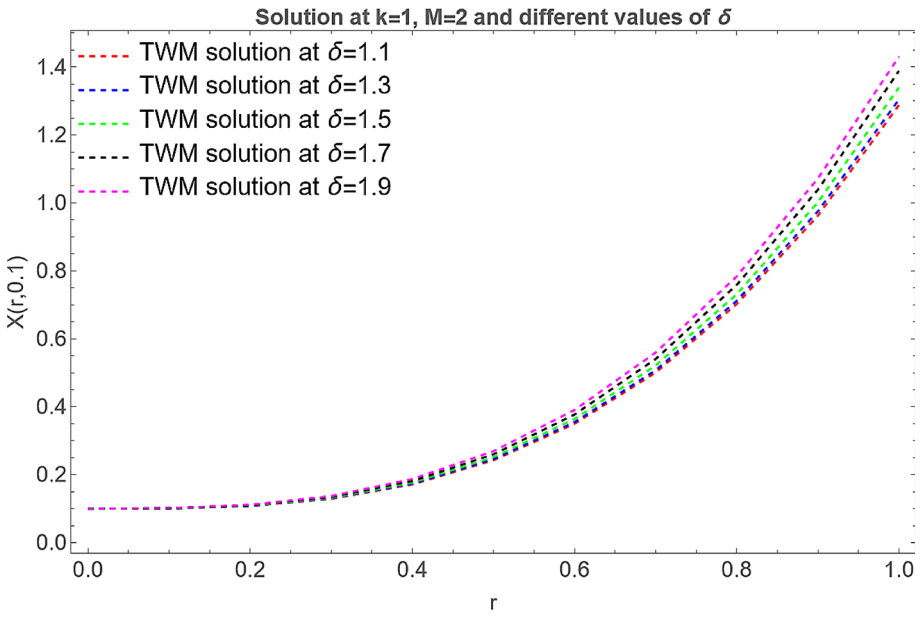

Fig. 9 Present method solution at $t = 0.1$ and different values of δ, for example, 6.2

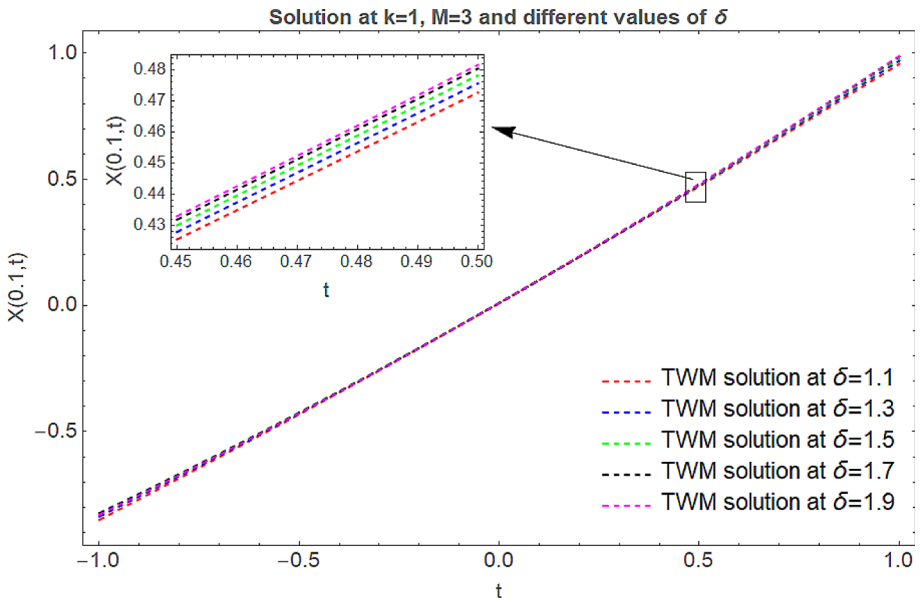

Fig. 10 Present method solution at $r = 0.1$ and different values of δ, for example, 6.2

Table 4 The comparison of different error norms of the projected method with different methods for $k = M = 3$ at different values of t and $\delta = 2$, for example, 6.2. (CPU time: 0.684 sec)

t	Taylor wavelet		Fibonacci wavelet [53]		Legendre wavelet [52]		Legendre wavelet [55]	
	L^∞	L^2	L^∞	L^2	L^∞	L^2	L^∞	L^2
0.1	1.52×10^{-18}	4.90×10^{-19}	4.24×10^{-17}	3.29×10^{-18}	2.22×10^{-16}	7.53×10^{-17}	4.90×10^{-3}	8.64×10^{-4}
0.3	5.38×10^{-18}	2.66×10^{-19}	6.16×10^{-17}	1.12×10^{-18}	1.11×10^{-16}	5.55×10^{-17}	1.47×10^{-3}	8.06×10^{-4}
0.5	3.19×10^{-18}	6.78×10^{-19}	0	0	1.11×10^{-16}	7.85×10^{-17}	2.28×10^{-3}	1.38×10^{-3}
0.7	2.86×10^{-18}	3.59×10^{-19}	0	0	2.22×10^{-16}	1.24×10^{-16}	1.17×10^{-3}	7.50×10^{-4}
0.9	7.27×10^{-18}	1.41×10^{-19}	3.77×10^{-17}	3.55×10^{-18}	4.44×10^{-16}	2.00×10^{-16}	6.45×10^{-3}	8.60×10^{-5}
1	0	0	0	0	2.22×10^{-16}	2.02×10^{-16}	0	0

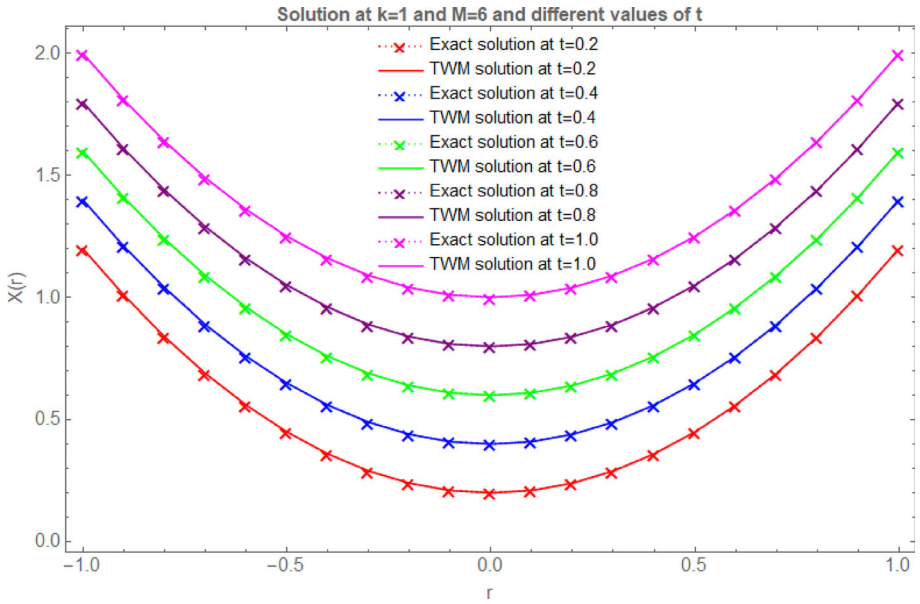

Fig. 11 Present method solution at different values of t, for example, 6.2

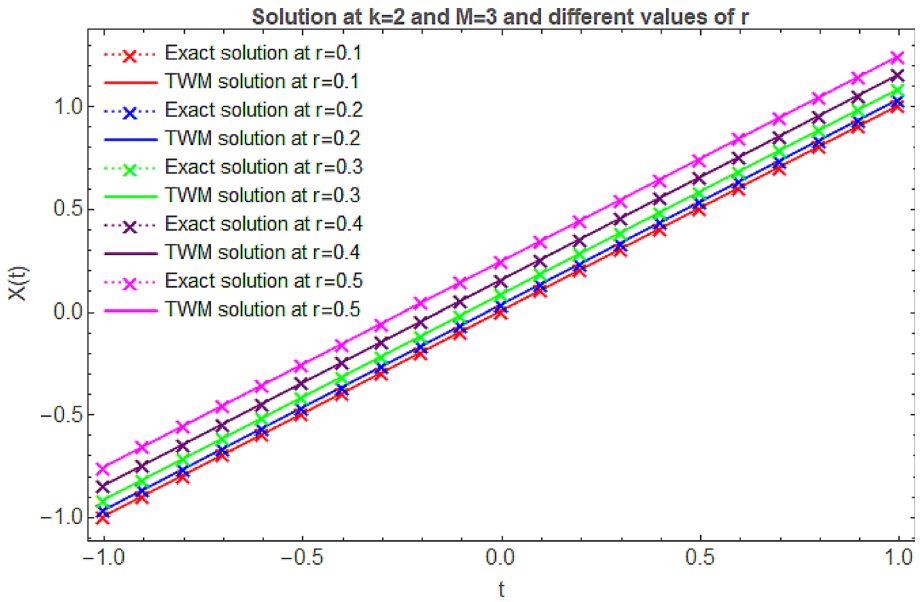

Fig. 12 Present method solution at different values of r, for example, 6.2

$$\frac{\partial X(r,\,t)}{\partial r} = \frac{\partial L_1(r)}{\partial r} + \frac{1}{c}[L_3(t) - L_2(t) - L_1(c) + L_1(0) - \lim_{r\to c}\left[\mathbb{B}\prime\lambda(r) + \bar{\lambda}(r)'\right]^T Q\left[\mathbb{B}\lambda(t) + \bar{\lambda}(t)\right]\Big] + \left[\mathbb{B}\lambda(r) + \bar{\lambda}(r)\right]^T Q\left[\mathbb{B}\lambda(t) + \bar{\lambda}(t)\right], \tag{5.8}$$

$$X(r,\,t) = L_2(t) + L_1(r) - L_1(0) + \left[\mathbb{B}\prime\lambda(r) + \bar{\lambda}(r)'\right]^T Q\left[\mathbb{B}\lambda(t) + \bar{\lambda}(t)\right] + \frac{r}{c}[L_3(t) - L_2(t) - L_1(c) + L_1(0) - \lim_{r\to c}\left[\mathbb{B}\prime\lambda(r) + \bar{\lambda}(r)'\right]^T Q\left[\mathbb{B}\lambda(t) + \bar{\lambda}(t)\right]\Big], \tag{5.9}$$

Case I: If $\delta = 2$ in Eq. (5.1), then differentiate Eq. (5.9) with concerning t. We obtain,

$$\frac{\partial^2 X(r,\,t)}{\partial t^2} = \frac{d^2}{dt^2}L_2(t) + \frac{r}{c}\frac{d^2}{dt^2}[L_3(t) - L_2(t) - L_1(c) + L_1(0)$$

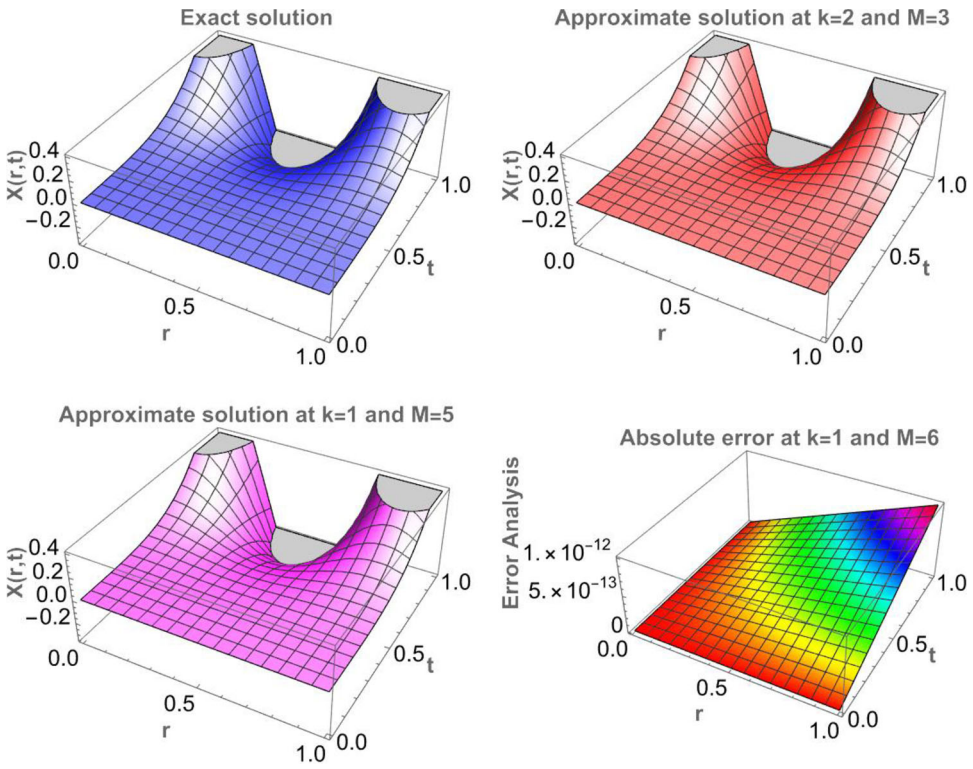

Fig. 13 The exact solution, approximate solution for different values of k and M, and an absolute error, for example, 6.3

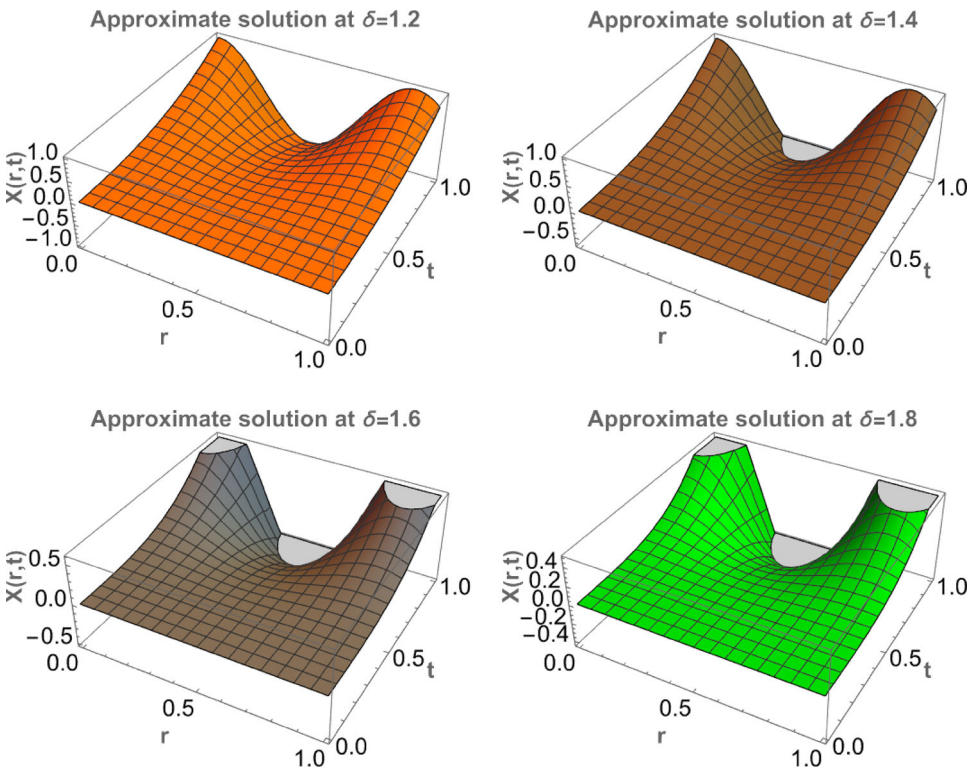

Fig. 14 Present method solution at $k = 2$, $M = 5$, and different values of δ, for example, 6.3

Table 5 The present method solution at $r = 0.1$, $k = 1$, $M = 4$, and different values of δ, for example, 6.3. (CPU time: 0.563 sec)

t	TWM				
	$\delta = 1.1$	$\delta = 1.3$	$\delta = 1.5$	$\delta = 1.7$	$\delta = 1.9$
0.1	0.00482582	0.00192119	0.00076484	0.00030448	0.00012121
0.2	0.02217368	0.01164795	0.00611873	0.00321420	0.00168844
0.3	0.05410514	0.03342620	0.02065073	0.01275804	0.00788193
0.4	0.10188349	0.07062001	0.04894989	0.03392937	0.02351796
0.5	0.16645844	0.12615191	0.09560527	0.07245524	0.05491081
0.6	0.24860198	0.20265862	0.16520591	0.13467472	0.10978590
0.7	0.34896954	0.30257060	0.26234087	0.22746007	0.19721701
0.8	0.46813359	0.42815971	0.39159919	0.35816058	0.32757728
0.9	0.60660411	0.58157048	0.55756995	0.53455988	0.51249941

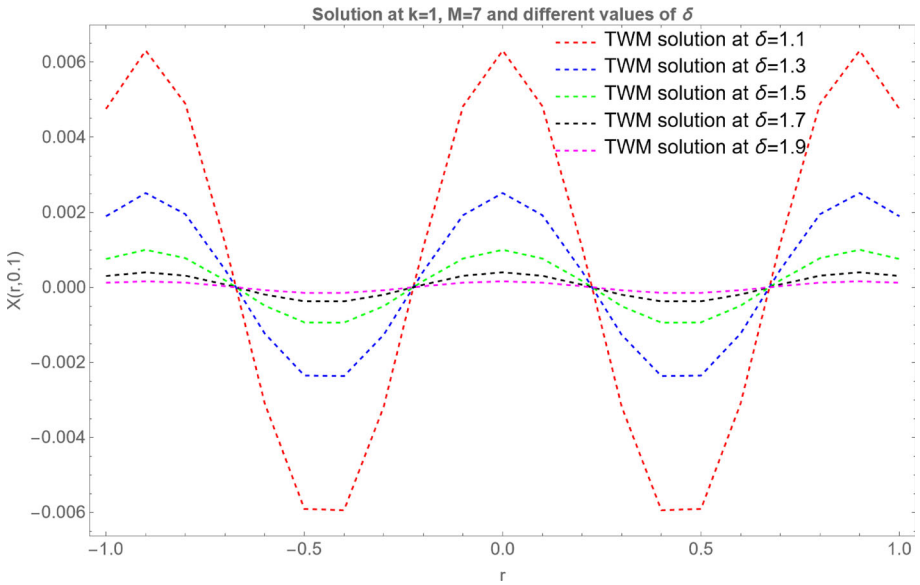

Fig. 15 Present method solution at $t = 0.1$ and different values of δ, for example, 6.3

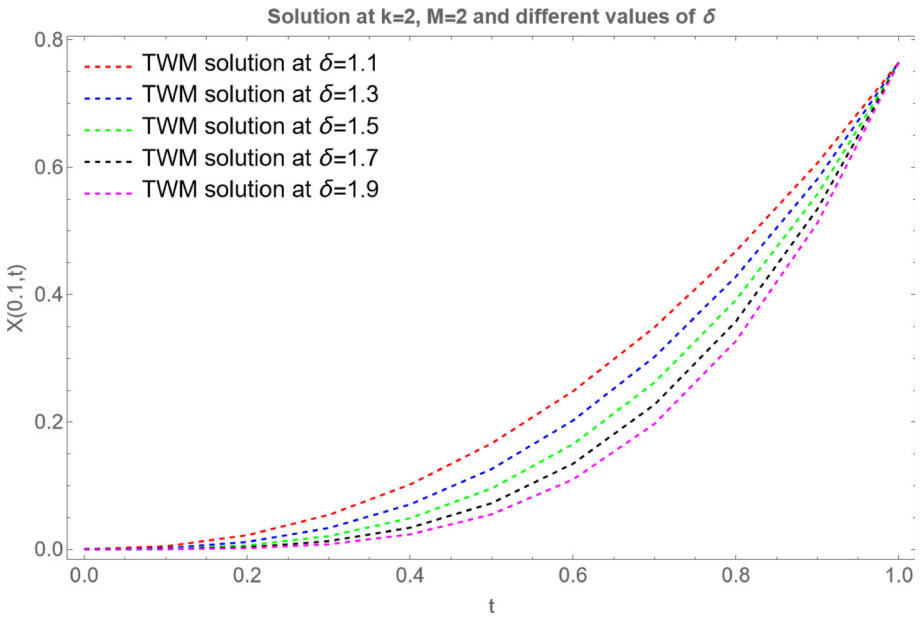

Fig. 16 Present method solution at $r = 0.1$ and different values of δ, for example, 6.3

Table 6 The comparison of absolute errors of the projected method with another method for $k = 2$, $M = 6$ at different values of δ, for example, 6.3. (CPU time: 0.670 sec)

(r, t)	$\delta = 1.25$		$\delta = 1.65$		$\delta = 1.95$	
	TWM	LWM [52]	TWM	LWM [52]	TWM	LWM [52]
(0.1,0.1)	7.4702×10^{-11}	6.5614×10^{-6}	8.0547×10^{-11}	2.3169×10^{-6}	7.9591×10^{-12}	3.8347×10^{-7}
(0.2,0.2)	3.0065×10^{-10}	4.1994×10^{-6}	3.5402×10^{-10}	6.1470×10^{-6}	2.2330×10^{-11}	2.3887×10^{-6}
(0.3,0.3)	6.8052×10^{-10}	1.1611×10^{-6}	8.6933×10^{-10}	6.3832×10^{-6}	6.9827×10^{-11}	4.4284×10^{-6}
(0.4,0.4)	1.2169×10^{-9}	6.9869×10^{-6}	9.6757×10^{-10}	5.2387×10^{-6}	1.0527×10^{-10}	4.7642×10^{-6}
(0.5,0.5)	1.9126×10^{-9}	9.0325×10^{-5}	2.8214×10^{-9}	8.8872×10^{-7}	1.9360×10^{-10}	1.9802×10^{-6}
(0.6,0.6)	2.7705×10^{-9}	8.3791×10^{-5}	4.3524×10^{-9}	1.9476×10^{-6}	2.6868×10^{-10}	2.0201×10^{-7}
(0.7,0.7)	3.7937×10^{-9}	6.2152×10^{-5}	6.3127×10^{-9}	5.0543×10^{-6}	5.0108×10^{-10}	1.8224×10^{-7}
(0.8,0.8)	4.9856×10^{-9}	4.4516×10^{-5}	8.7452×10^{-9}	9.0031×10^{-6}	6.5805×10^{-10}	2.8284×10^{-6}
(0.9,0.9)	6.3493×10^{-9}	5.5285×10^{-5}	1.1693×10^{-8}	2.2000×10^{-5}	9.0351×10^{-10}	1.5856×10^{-5}

$$- \lim_{r \to c} \left[\mathbb{B}\prime\lambda(r) + \bar{\lambda}(r)' \right]^T Q \left[\mathbb{B}\lambda(t) + \bar{\lambda}(t) \right] \Bigg] + \frac{d^2}{dt^2} \left[\left[\mathbb{B}\prime\lambda(r) + \bar{\lambda}(r)' \right]^T Q \left[\mathbb{B}\lambda(t) + \bar{\lambda}(t) \right] \right], \tag{5.10}$$

Now fit the X, X_t, X_{tt}, X_r, and X_{rr} into Eq. (5.1), and discretise with their respective collocation points in Eq. (5.11).

$$r_i = t_i = \frac{2i-1}{2^k[M]^2},\ i = 1, 2, \ldots, 2^{k-1}[M]^2. \tag{5.11}$$

We solve the system of algebraic equations using the Newton–Raphson method to ascertain the values of the unknown coefficients. In Eq. (5.9), substitute the obtained values of the unknown coefficients to get the deserved approximate solution for the given PDE.

Case II: Utilizing the notion of Caputo derivative, which is defined in Sect. 2.1, differentiate Eq. (5.9) fractionally of order $\delta \in (1, 2)$ for the given equation. Then we obtain,

$$\begin{aligned} \frac{\partial^\delta X(r,t)}{\partial t^\delta} &= \frac{d^\delta}{dt^\delta} L_2(t) \\ &+ \frac{r}{c} \frac{d^\delta}{dt^\delta} \Bigg[L_3(t) - L_2(t) - L_1(c) + L_1(0) \\ &- \lim_{r \to c} \left[\mathbb{B}'\lambda(r) + \overline{\lambda(r)}' \right]^T Q \left[\lambda\mathbb{B}(t) + \overline{\lambda(t)} \right] \Bigg] \\ &+ \frac{d^\delta}{dt^\delta} \left[\left[\mathbb{B}'\lambda(r) + \overline{\lambda(r)}' \right]^T Q \left[\mathbb{B}\lambda(t) + \overline{\lambda(t)} \right] \right] \end{aligned} \tag{5.12}$$

To collocate with the collocation points $r_i = t_i = \frac{2i-1}{2^k[M]^2}$, $i = 1, 2, \ldots, 2^{k-1}[M]^2$, by replacing X, $\frac{\partial^{\delta-1} X(r,t)}{\partial t^{\delta-1}}$, $\frac{\partial^\delta X(r,t)}{\partial t^\delta}$, X_r, and X_{rr} in (5.1). For finding the unknown coefficients by applying the Newton–Raphson method to the obtained system of algebraic equations. Substitute the calculated values for the unknown coefficients in Eq. (5.9), which produces the desired solution of the proposed method.

6 Numerical experiments

The error norms can be demonstrated as

$$L^2\text{error} = \sqrt{\sum_{i=1}^{n} Z_i^2},\ L^\infty\text{error} = \text{Max}(Z_i),\ 1 \le i \le n-1$$

where $Z_i(\text{absoluteerror}) = X_i(\text{exactsolution}) - X_i(\text{approximatesolution})$.

We utilized Mathematica 13.2.1 software in a laptop with the configuration HP-i5, 11th generation, 8 GB RAM, and 512 GB SSD.

Example 6.1 Consider the time-fractional telegraph equation [52].

$$\frac{\partial^\delta X(r,t)}{\partial t^\delta} + \frac{\partial^{\delta-1} X(r,t)}{\partial t^{\delta-1}} + X(r,t) = \frac{\partial^2 X(r,t)}{\partial r^2} + h(r,t),\ 1 < \delta \le 2$$

with initial and Dirichlet boundary conditions

$$X(r,0) = 0, \quad X_t(r,0) = r(r-1), \quad 0 \le r \le 1,$$

$$X(0,t) = 0, \quad X(1,t) = 0, \quad 0 < t \le 1,$$

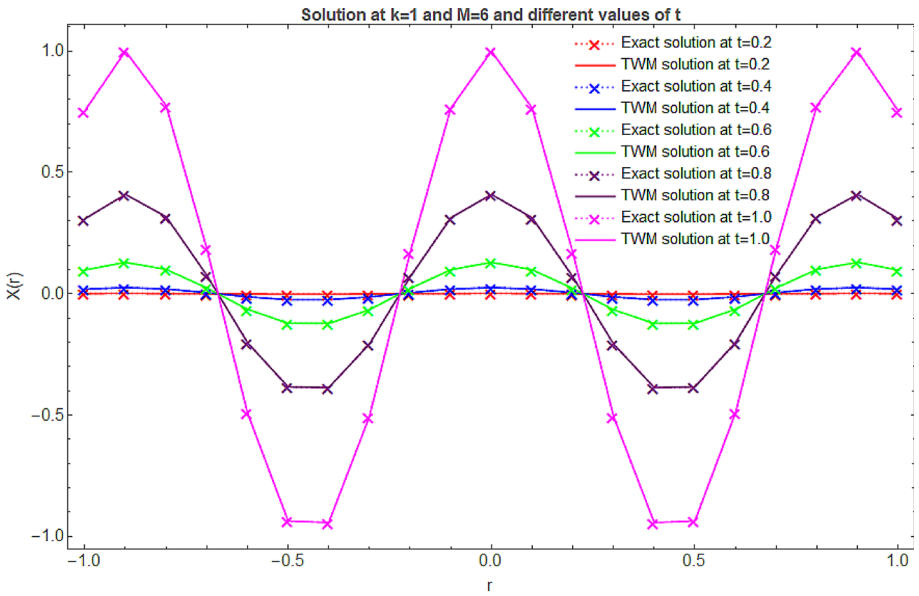

Fig. 17 Present method solution at different values of t, for example, 6.3

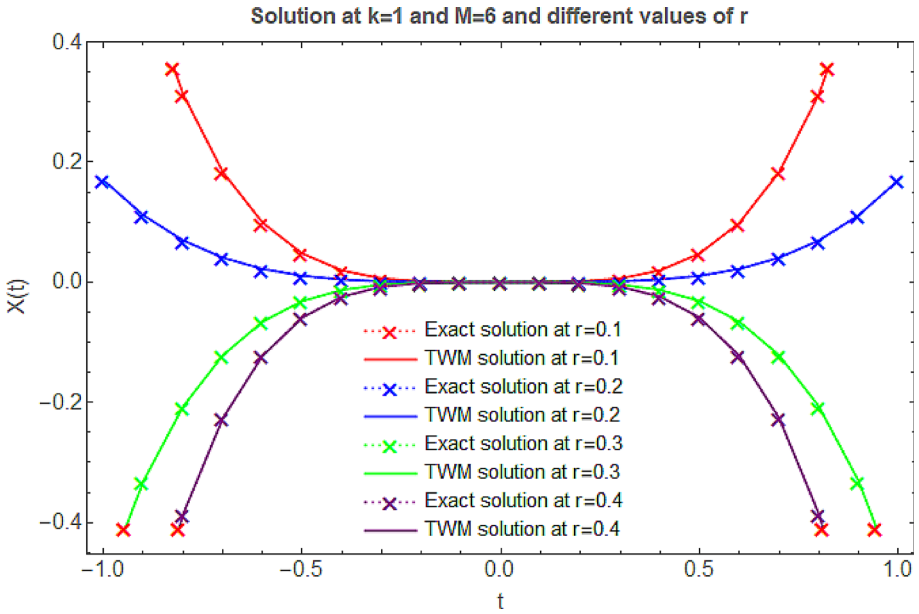

Fig. 18 Present method solution at different values of r, for example, 6.3

where

$$h(r,\, t) = \left(\frac{\Gamma(2)}{\Gamma(3-\delta)}t^{2-\delta} + t\right)\left(r^2 - r\right) - 2t.$$

The exact solution of this telegraph equation is $X(r,\, t) = \left(r^2 - r\right)t$. The projected technique is the Taylor wavelet method. Figure 1 represents a 3-dimensional graphical illustration of the exact solution, the projected method solution for different values of k and M, and the absolute error analysis graph plotted. Figure 2 denotes a 3-dimensional graph of the current method solution for different values of δ. Table 1 expresses the TWM solution at $r = 0.1$ and for different values of δ. Figures 3 and 4 show the graphical demonstration of the present method solution at $t = 0.1$ and $r = 0.1$, respectively, for different values of δ. Table 2 reveals the accuracy of the method solution is directly proportional to the values of k and M. The accuracy of the solution increases by increasing the values of k and M. Table 2 compares the absolute errors of the present method with the Legendre [52], Fibonacci [53], and the Sinc-Legendre wavelet method [54]. Figures 5 and 6 display graphs of the TWM solution for different values of t and r, respectively.

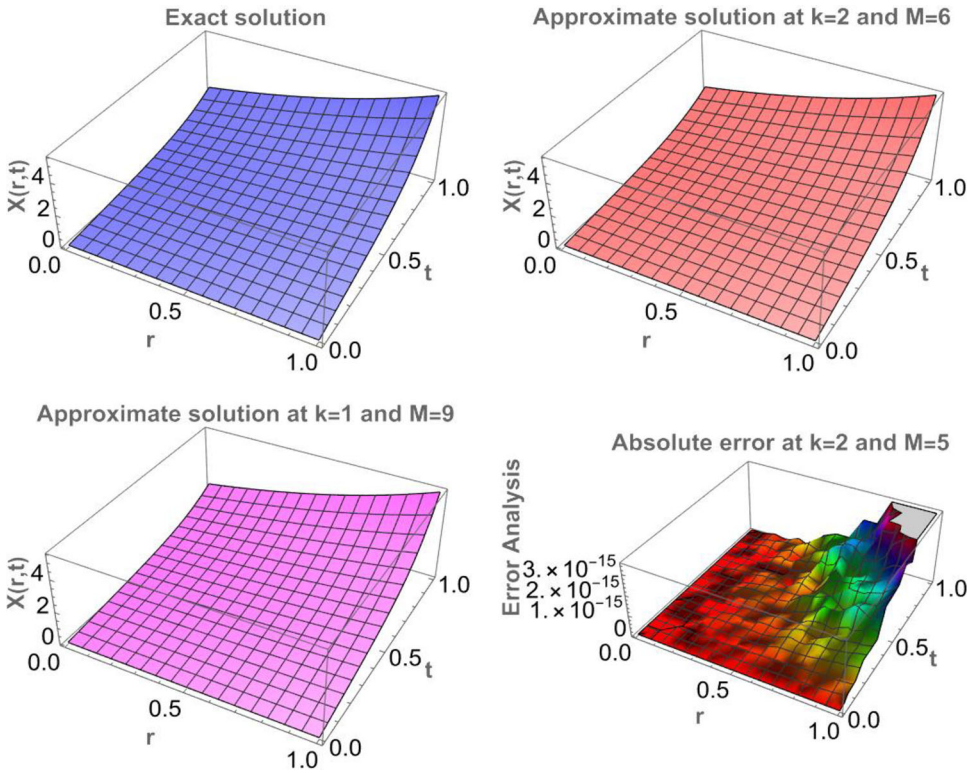

Fig. 19 The exact solution, approximate solution for different values of k and M, and an absolute error, for example, 6.4

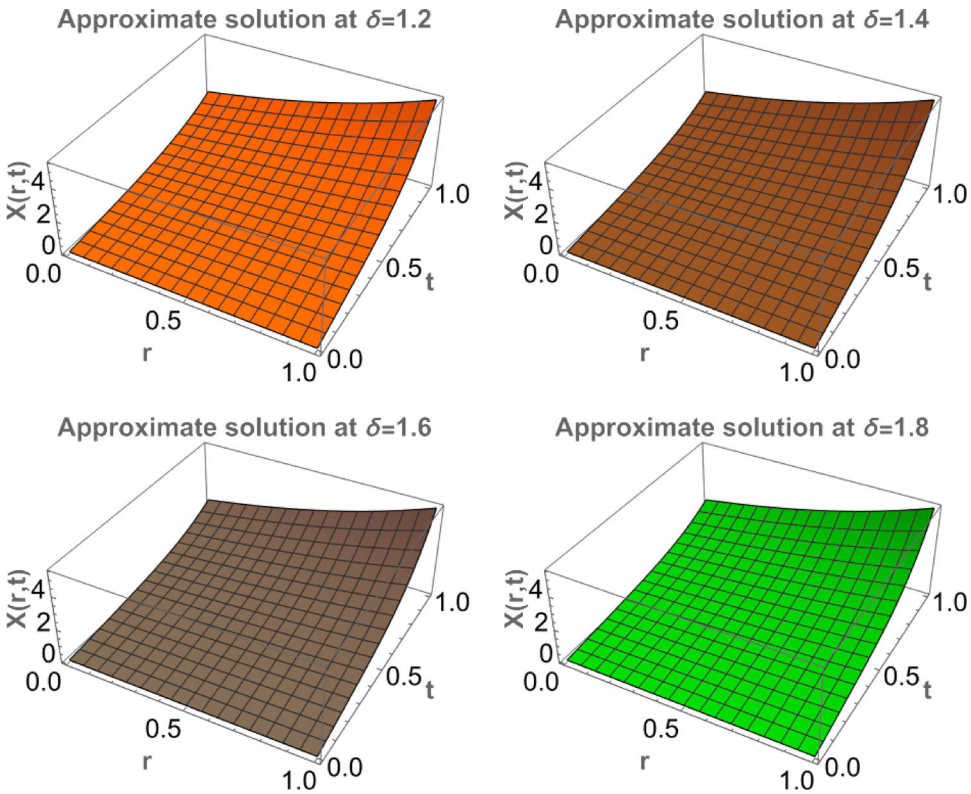

Fig. 20 Present method solution at $k = 1$, $M = 8$, and different values of δ, for example, 6.4

Table 7 The present method solution at $r = 0.1$, $k = 1$, $M = 4$, and for different values of δ, for example, 6.4. (CPU time: 0.597 sec)

t	TWM				
	$\delta = 1.1$	$\delta = 1.3$	$\delta = 1.5$	$\delta = 1.7$	$\delta = 1.9$
0.1	0.11060487	0.11057248	0.11055204	0.11053914	0.11053100
0.2	0.22253958	0.22212526	0.22182497	0.22160733	0.22144959
0.3	0.33948773	0.33778935	0.33645442	0.33540516	0.33458044
0.4	0.46788356	0.46356089	0.45996203	0.45696579	0.45447127
0.5	0.61703301	0.60869031	0.60142757	0.59510499	0.58960086
0.6	0.79919987	0.78598216	0.77404814	0.76327316	0.75354463
0.7	1.02967355	1.01204421	0.99562866	0.98034332	0.96611038
0.8	1.32682539	1.30750313	1.28902425	1.27135192	1.25445095
0.9	1.71215685	1.69719573	1.68254658	1.66820289	1.65415829

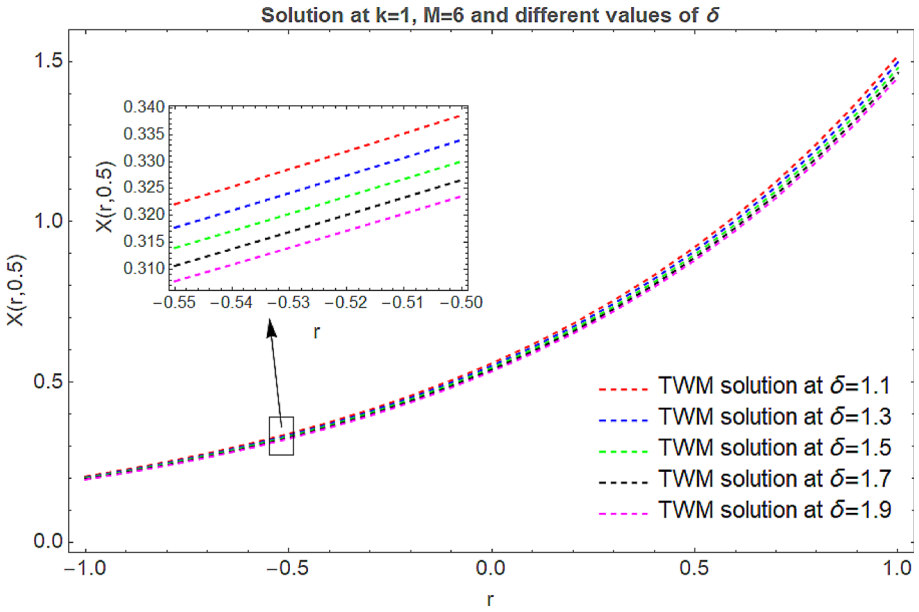

Fig. 21 Present method solution at $t = 0.5$ and different values of δ, for example, 6.4

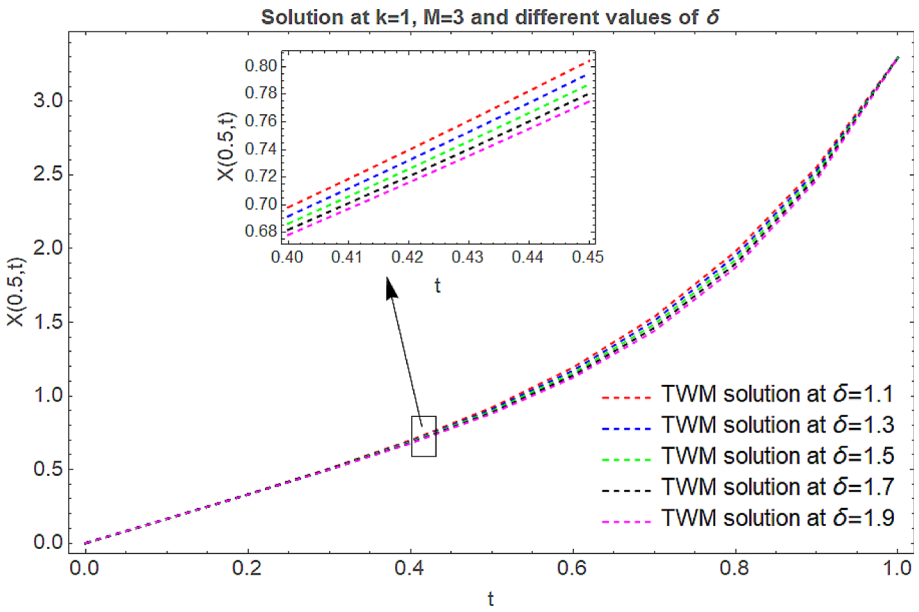

Fig. 22 Present method solution at $r = 0.5$ and different values of δ, for example, 6.4

Table 8 The comparison of absolute errors of the projected method with another method for $k = 2$, $M = 6$ at different values of δ, for example, 6.4. (CPU time: 0.667 sec)

(r, t)	$\delta = 1.1$		$\delta = 1.5$		$\delta = 1.9$	
	TWM	LWM [52]	TWM	LWM [52]	TWM	LWM [52]
(0.1,0.1)	1.6751×10^{-15}	1.3531×10^{-9}	4.1961×10^{-15}	1.6883×10^{-8}	2.0961×10^{-15}	1.7955×10^{-8}
(0.2,0.2)	7.1023×10^{-15}	1.3283×10^{-9}	1.7597×10^{-14}	2.6116×10^{-8}	8.8237×10^{-15}	5.1220×10^{-8}
(0.3,0.3)	1.6867×10^{-14}	3.2054×10^{-9}	4.1336×10^{-14}	2.1232×10^{-8}	2.0756×10^{-14}	8.5286×10^{-8}
(0.4,0.4)	3.1532×10^{-14}	2.3944×10^{-9}	7.6426×10^{-14}	2.2362×10^{-8}	3.8346×10^{-14}	1.0671×10^{-7}
(0.5,0.5)	5.1630×10^{-14}	9.5664×10^{-8}	1.2374×10^{-13}	3.3459×10^{-8}	6.1908×10^{-14}	9.8781×10^{-8}
(0.6,0.6)	7.7667×10^{-14}	1.1048×10^{-7}	1.8401×10^{-13}	2.3240×10^{-7}	9.1610×10^{-14}	1.0213×10^{-7}
(0.7,0.7)	1.1011×10^{-13}	4.1133×10^{-8}	3.5780×10^{-13}	1.9078×10^{-7}	1.2745×10^{-13}	8.4231×10^{-8}
(0.8,0.8)	1.4940×10^{-13}	2.3961×10^{-9}	5.4548×10^{-13}	9.9970×10^{-8}	1.6925×10^{-13}	5.1459×10^{-8}
(0.9,0.9)	1.9593×10^{-13}	2.1296×10^{-8}	4.9724×10^{-13}	3.1380×10^{-8}	2.1664×10^{-13}	1.8774×10^{-8}

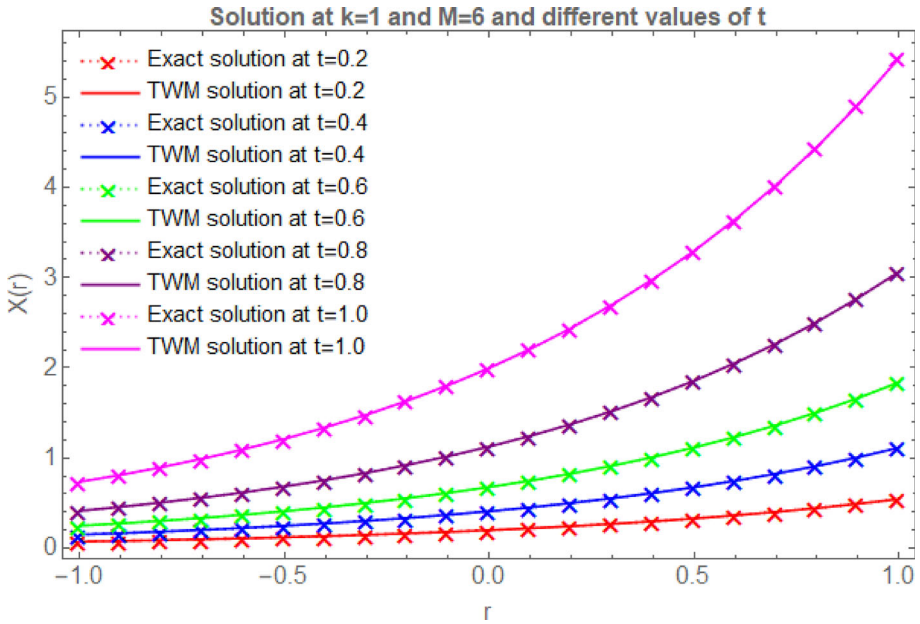

Fig. 23 Present method solution at different values of t, for example, 6.4

Example 6.2 Consider the time-fractional telegraph equation [52].

$$\frac{\partial^{\delta} X(r, t)}{\partial t^{\delta}} + \frac{\partial^{\delta-1} X(r, t)}{\partial t^{\delta-1}} + X(r, t) = \frac{\partial^2 X(r, t)}{\partial r^2} + h(r, t), \ 1 < \delta \leq 2$$

with initial and Dirichlet boundary conditions

$$X(r, 0) = r^2, \quad X_t(r, 0) = 1 + r^2, \quad 0 \leq r \leq 1,$$

$$X(0, t) = t, \quad X(1, t) = 1 + t, \quad 0 < t \leq 1,$$

where

$$h(r, t) = \frac{\Gamma(2)}{\Gamma(3-\delta)} + r^2 + t - 2.$$

The exact solution of this telegraph equation is $X(r, t) = r^2 + t$. Figure 7 gives a 3-dimensional graphical presentation of the exact solution, approximate solution, and error analysis. Figure 8 is a 3-dimensional graph of the TWM solution for different δ values. Table 3 confirms the projected technique solution to the different δ values. Figures 9 and 10 show the graphical judgment of the present method solution at $t = 0.1$ and $r = 0.1$, respectively, for different δ values. Table 4 compares the L^{∞} and L^2 error norms of the projected method with the Legendre [52, 55] and Fibonacci wavelet method [53] at different values of t. Figures 11 and 12 exhibit the graphical interpretation of the current method solution for different values of t and r, respectively.

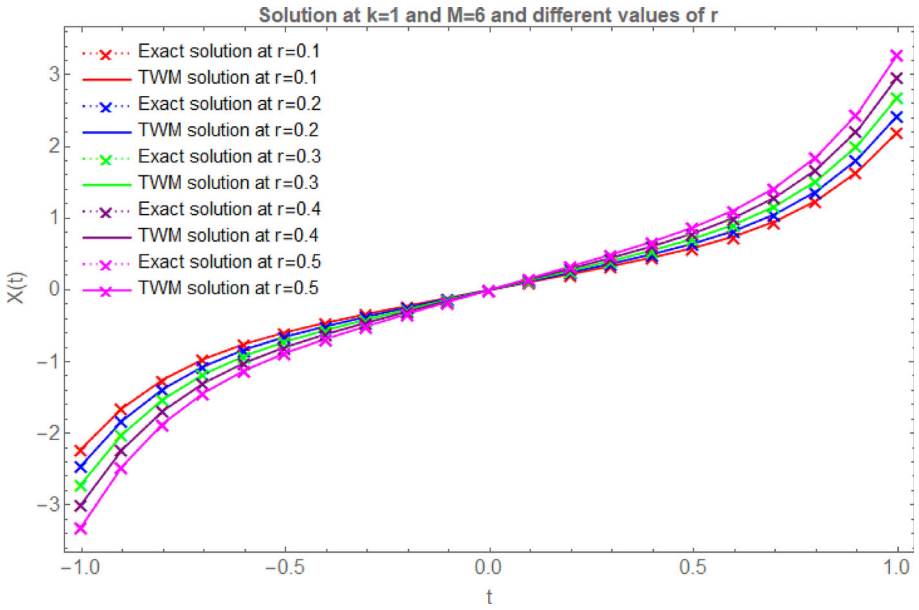

Fig. 24 Present method solution at different values of r, for example, 6.4

Example 6.3 Consider the time-fractional telegraph equation [52].

$$\frac{\partial^{\delta} X(r,t)}{\partial t^{\delta}} + \frac{\partial^{\delta-1} X(r,t)}{\partial t^{\delta-1}} + X(r,t) = \frac{\partial^2 X(r,t)}{\partial r^2} + h(r,t), \ 1 < \delta \leq 2$$

with initial and Dirichlet boundary conditions

$$X(r,0) = 0, \quad X_t(r,0) = 0, \quad 0 \leq r \leq 1,$$

$$X(0,t) = t^{2\delta}, \quad X(1,t) = \cos(7)t^{2\delta}, \quad 0 < t \leq 1,$$

where

$$h(r,t) = \left(\frac{\Gamma(2\delta+1)}{\Gamma(\delta+1)}t^{\delta} + \frac{\Gamma(2\delta+1)}{\Gamma(\delta+2)}t^{\delta+1} + 50t^{2\delta}\right)\cos(7r).$$

The exact solution of this telegraph equation is $X(r,t) = \cos(7r)t^{2\delta}$. Figure 13 determines the 3-dimensional graphical comparison of the analytical and Taylor wavelet solutions, and the absolute error graph is also drawn. Figure 14 confirms the 3-dimensional graphical illustration of different values of δ. Table 5 explains the present method solution for different values of δ. Figures 15 and 16 elucidate the current technique solution for different values of δ at $t = 0.1$ and $r = 0.1$, respectively. Table 6 compares the present method with the Legendre wavelet method (LWM) [52] for different points of δ. Figures 17 and 18 describe the graphical illustration of the current method solution for different values of t and r, respectively.

Example 6.4 Consider the time-fractional telegraph equation [52].

$$\frac{\partial^{\delta} X(r,t)}{\partial t^{\delta}} + \frac{\partial^{\delta-1} X(r,t)}{\partial t^{\delta-1}} + X(r,t) = \frac{\partial^2 X(r,t)}{\partial r^2} + h(r,t), \ 1 < \delta \leq 2$$

with initial and Dirichlet boundary conditions

$$X(r,0) = 0, \quad X_t(r,0) = e^r, \quad 0 \leq r \leq 1,$$

$$X(0,t) = t^{\delta+3} + t, \quad X(1,t) = (t^{\delta+3} + t)e, \quad 0 < t \leq 1,$$

where

$$h(r,t) = \left(\frac{\Gamma(\delta+4)}{\Gamma(4)}t^3 + \frac{\Gamma(\delta+4)}{\Gamma(5)}t^4 + \frac{\Gamma(2)}{\Gamma(3-\delta)}t^{2-\delta}\right)e^r.$$

The exact solution of this telegraph equation is $X(r,t) = (t^{\delta+3} + t)e^r$. Figure 19 shows a 3-dimensional graphical presentation of the exact solution, approximate solution, and error analysis at different values of k and M. Figure 20 is a 3-dimensional graphical diagram of the TWM solution for different δ values. Table 7 confirms the projected technique solution to the different δ values. Figures 21 and 22 show the graphical interpretation of the present method solution at $t = 0.1$ and $r = 0.1$, respectively, for different δ values. Table 8 compares the present method with LWM [52] for different points of δ. Figures 23 and 24 exhibit the graphical representation of the current method solution for different values of t and r, respectively.

7 Conclusion

This work developed an effective wavelet method based on Taylor wavelets to investigate the nonhomogeneous time-fractional telegraph Eq. (1.1) with Dirichlet boundary conditions. We took a collocation-based strategy. The novel technique on Taylor wavelets is applied to four problems. The approach is quite easy for handling boundary value problems. The tables and graphs explain the behavior of telegraph equations and show the method's accuracy is good compared to other literature methods. A small resolution level in the suggested method ensures the required precision. By the tables and graphs, we conclude that the present method's accuracy is directly proportional to the values of k and M. From comparison in the tables, the present technique has higher precision for similar series terms than other methods. The effectiveness and adaptability of the suggested method in comparison to other methods available in the literature [52–55] and good agreement with the analytical solutions were demonstrated through numerical experiments. Finally, we conclude that the TWM is highly robust, straightforward, and effective in generating numerical solutions to various fractional partial differential equations-related problems in physics, mathematics, and engineering. With minor modifications to the method, the current approach can be extended to models with higher-order PDEs, higher-order fractional PDEs, time-delay PDEs, and systems of PDEs.

Acknowledgements The authors are grateful to the referees and the editor for carefully checking the details and for helpful comments that improved this paper. The author expresses his affectionate thanks to the DST-SERB, Govt. of India, New Delhi, for the financial support under Empowerment and Equity Opportunities for Excellence in Science for 2023-2026. F.No.EEQ/2022/620 Dated:07/02/2023.

Author contributions The manuscript was written through contributions of both authors. Both authors have given approval to the final version of the manuscript.

Funding The authors state that no funding is involved.

Data Availability The data supporting this study's findings are available within the article.

Code Availability None.

Declarations

Conflict of Interest The authors have no competing interests to declare that are relevant to the content of this article.

References

1. Podlubny I (1999) Fractional differential equations. Academic Press, San Diego
2. Atangana A, Baleanu D (2016) New fractional derivatives with nonlocal and nonsingular kernel: theory and application to heat transfer model. Therm Sci 20(2):763–769. https://doi.org/10.2298/TSCI160111018A
3. Caputo M, Fabrizio M (2015) A new definition of fractional derivative without singular kernel. Progress Fract Diff Appl 1(2):73–85
4. Kilbas AA, Srivastava HM, Trujillo JJ (2006) Theory and applications of fractional differential equations. Elsevier, London, p 204
5. Chen W, Sun HG, Zhang XD, Korosak D (2010) Anomalous diffusion modeling by fractal and fractional derivatives. Comput Math Appl 59(5):1754–1758. https://doi.org/10.1016/j.camwa.2009.08.020
6. Baleanu D, Jajarmi A, Mohammadi H, Rezapour S (2020) A new study on the mathematical modelling of human liver with Caputo-Fabrizio fractional derivative. Chaos, Solitons Fractals 134:109705. https://doi.org/10.1016/j.chaos.2020.109705
7. Hassani H, Naraghirad E (2019) A new computational method based on optimization scheme for solving variable-order time fractional Burgers' equation. Math Comput Simul 162:1–17. https://doi.org/10.1016/j.matcom.2019.01.002
8. Chen W (2006) A speculative study of 2/3-order fractional Laplacian modeling of turbulence: some thoughts and conjectures. Chaos 16(2):023126. https://doi.org/10.1063/1.2208452
9. Khan MA, Atangana A (2019) Dynamics of Ebola disease in the framework of different fractional derivatives. Entropy 21(3):303. https://doi.org/10.3390/e21030303
10. Hall MG, Barrick TR (2008) From difusion-weighted MRI to anomalous difusion imaging. Magn Reson Med 59(3):447–455. https://doi.org/10.1002/mrm.21453
11. Ghanbari B, Atangana A (2020) A new application of fractional Atangana-Baleanu derivatives: designing ABC-fractional masks in image processing. Physica A 542:123516. https://doi.org/10.1016/j.physa.2019.123516
12. Khirsariya SR, Rao SB, Chauhan JP (2022) Semi-analytic solution of time-fractional Korteweg-de Vries equation using fractional residual power series method. Results Nonlinear Anal 5(3):222–234
13. Khirsariya SR, Rao SB, Chauhan JP (2023) A novel hybrid technique to obtain the solution of generalized fractional-order differential equations. Math Comput Simul 205:272–290. https://doi.org/10.1016/j.matcom.2022.10.013
14. Khirsariya SR, Rao SB (2023) On the semi-analytic technique to deal with nonlinear fractional differential equations. J Appl Math Comput Mech 22(1):17–30
15. Khirsariya SR, Rao SB (2023) Solution of fractional Sawada–Kotera–Ito equation using Caputo and Atangana-Baleanu derivatives. Math Methods Appl Sci. https://doi.org/10.1002/mma.9438
16. Hunt BJ (1994) The Maxwellians. Cornell University Press, New York
17. Raines JK (2007) Folded Unipole Antennas: Theory and applications. McGraw Hill, London
18. Schelkunoff SA, Friis HT (1952) Antennas: Theory and practice. John Wiley & Sons, Newyork
19. Pascal H (1986) Pressure wave propagation in a fluid flowing through a porous medium and problems related to interpretation of Stoneley wave at tenuation in acoustical well logging. Int J Eng Sci 24(9):1553–1570. https://doi.org/10.1016/0020-7225(86)90163-1
20. Jordan PM, Puri A (1999) Digital signal propagation in dispersive media. J Appl Phys 85(3):1273–1282. https://doi.org/10.1063/1.369258
21. Holmes EE (1993) Are diffusion models too simple? A comparison with telegraph models of invasion. Am Nat 142(5):779–795. https://doi.org/10.1086/285572
22. Bohme G (1987) Non-newtonian fluid mechanics. North-Holland, New York

23. Barletta A, Zanchini E (1999) A thermal potential for mulation of hyperbolic heat conduction. ASME J Heat Mass Transfer 121(1):166–169. https://doi.org/10.1115/1.2825933
24. Debnath L (1997) Non-linear partial differential equations for scientists and engineers. Birkhäuser, Bostan
25. Razzaghi M, Yousef S (2001) The Legendre wavelets operational matrix of integration. Int J Syst Sci 32(4):495–502. https://doi.org/10.1080/00207720120227
26. Beylkin G, Coifman R, Rokhlin V (1991) Fast wavelet transforms and numerical algorithms I. Commun Pure Appl Math 44(2):141–183. https://doi.org/10.1002/cpa.3160440202
27. Kumbinarasaiah S, Mulimani M (2022) A novel scheme for the hyperbolic partial differential equation through Fibonacci wavelets. J Taibah Univ Sci 16(1):1112–1132. https://doi.org/10.1080/16583655.2022.2143636
28. Kumbinarasaiah S, Mulimani M (2023) Fibonacci wavelets-based numerical method for solving fractional order (1 + 1)-dimensional dispersive partial differential equation. Int J Dyn Control 11:2232–2255. https://doi.org/10.1007/s40435-023-01129-1
29. Hussain B, Afroz A, Jahan S (2021) Approximate solution for proportional-delay riccati differential equations by Haar wavelet method. Poincare J Anal Appl 8(2):157–170
30. Yadav P, Jahan S, Nisar KS (2023) Solving fractional Bagley-Torvik equation by fractional order Fibonacci wavelet arising in fluid mechanics. Ain Shams Eng J. https://doi.org/10.1016/j.asej.2023.102299
31. Yadav P, Jahan S, Nisar KS (2023) Fibonacci wavelet collocation method for fredholm integral equations of second kind. Qual Theory Dyn Syst 22:82. https://doi.org/10.1007/s12346-023-00785-0
32. Ahmed S, Jahan S, Nisar KS (2023) Hybrid Fibonacci wavelet method to solve fractional-order logistic growth model. Math Methods Appl Sci. https://doi.org/10.1002/mma.9446
33. Ahmed S, Shah K, Jahan S, Abdeljawad T (2023) An efficient method for the fractional electric circuits based on Fibonacci wavelet. Results in Physics 52:106753. https://doi.org/10.1016/j.rinp.2023.106753
34. Faheem M, Raza A, Khan A (2022) Wavelet collocation methods for solving neutral delay differential equations. Int J Nonlinear Sci Num Simulat 23(7–8):1129–1156. https://doi.org/10.1515/ijnsns-2020-0103
35. Kumbinarasaiah S, Raghunatha KR, Preetham MP (2023) Applications of Bernoulli wavelet collocation method in the analysis of Jeffery-Hamel flow and heat transfer in Eyring-Powell fluid. J Therm Anal Calorim 148:1173–1189. https://doi.org/10.1007/s10973-022-11706-9
36. Li F, Baskonus HM, Kumbinarasaiah S, Manohara G, Gao W, Ilahan E (2023) An efficient numerical scheme for biological models in the frame of bernoulli wavelets. Comput Model Eng Sci. https://doi.org/10.32604/cmes.2023.028069
37. Kumbinarasaiah S, Manohara G, Hariharan G (2023) Bernoulli wavelets functional matrix technique for a system of nonlinear singular Lane Emden equations. Math Comput Simul 204:133–165. https://doi.org/10.1016/j.matcom.2022.07.024
38. Kumbinarasaiah S, Mulimani M (2023) A study on the non-linear murray equation through the bernoulli wavelet approach. Int J Appl Comput Math 9(3):40. https://doi.org/10.1007/s40819-023-01500-y
39. Chowdhury MSH, Aznam SM (2018) Generalized Haar wavelet operational matrix method for solving hyperbolic heat conduction in thin surface layers. Results Phys 11:243–252. https://doi.org/10.1016/j.rinp.2018.08.021
40. Shiralashetti SC, Kumbinarasaiah S (2018) Cardinal B-spline wavelet based numerical method for the solution of generalized burgers-huxley equation. Int J Appl Comput Math 4:73. https://doi.org/10.1007/s40819-018-0505-y
41. Keshavarz E, Ordokhani Y, Razzaghi M (2018) The Taylor wavelets method for solving the initial and boundary value problems of Bratu-type equations. Appl Numer Math 128:205–216. https://doi.org/10.1016/j.apnum.2018.02.001
42. Yuttanan B, Razzaghi M, Vo TN (2021) A fractional-order generalized Taylor wavelet method for nonlinear fractional delay and nonlinear fractional pantograph differential equations. Math Methods Appl Sci 44(5):4156–4175. https://doi.org/10.1002/mma.7020
43. Vo TN, Razzaghi M, Toan PT (2022) Fractional-order generalized Taylor wavelet method for systems of nonlinear fractional differential equations with application to human respiratory syncytial virus infection. Soft Comput 26:165–173. https://doi.org/10.1007/s00500-021-06436-3
44. Toan PT, Vo TN, Razzaghi M (2021) Taylor wavelet method for fractional delay differential equations. Eng Comput 37:231–240. https://doi.org/10.1007/s00366-019-00818-w
45. Korkut SÖ (2023) An accurate and efficient numerical solution for the generalized burgers-huxley equation via taylor wavelets method: qualitative analyses and applications. Math Comput Simul 209:324–341. https://doi.org/10.1016/j.matcom.2023.02.019
46. Keshavarz E, Ordokhani Y (2019) A fast numerical algorithm based on the Taylor wavelets for solving the fractional integro-differential equations with weakly singular kernels. Math Methods Appl Sci 42(13):4427–4443. https://doi.org/10.1002/mma.5663
47. Gümgüm S (2020) Taylor wavelet solution of linear and nonlinear Lane-Emden equations. Appl Numer Math 158:44–53. https://doi.org/10.1016/j.apnum.2020.07.019
48. Aghazadeh N, Mohammadi A, Tanoglu G (2022) Taylor wavelets collocation technique for solving fractional nonlinear singular PDEs. Math Sci. https://doi.org/10.1007/s40096-022-00483-z
49. Sumathi V, Hemalatha S, Sripathy B (2022) The Taylor wavelets method for the numerical solution of nonlinear coupled reaction-diffusion equation in chemical engineering. AIP Conf Proc 2464(1):050002. https://doi.org/10.1063/5.0083902
50. Behera S, Ray SS (2022) A wavelet-based novel technique for linear and nonlinear fractional Volterra-Fredholm integro-differential equations. Comput Appl Math 41:77. https://doi.org/10.1007/s40314-022-01772-y
51. Kumbinarasaiah S, Mulimani M (2023) Fibonacci wavelets approach for the fractional Rosenau-Hyman equations. Results Control Opt 11:100221. https://doi.org/10.1016/j.rico.2023.100221
52. Xu X, Xu D (2018) Legendre wavelets direct method for the numerical solution of time-fractional order telegraph equations. Mediterr J Math 15:27. https://doi.org/10.1007/s00009-018-1074-3
53. Shah FA, Irfan M, Nisar KS, Matoog RT, Mahmoud EE (2021) Fibonacci wavelet method for solving time-fractional telegraph equations with Dirichlet boundary conditions. Results Phys 24:104123. https://doi.org/10.1016/j.rinp.2021.104123
54. Sweilam NH, Nagy AM, El-Sayed AA (2016) Solving time-fractional order telegraph equation via sinc-legendre collocation method. Mediterr J Math 13:5119–5133. https://doi.org/10.1007/s00009-016-0796-3
55. Heydari MH, Hooshmandasl MR, Mohammadi F (2014) Two-dimensional legendre wavelets for solving time-fractional telegraph equation. Adv Appl Math Mech 6(2):247–260. https://doi.org/10.4208/aamm.12-m12132